ABSTRACT

Title of Document:	STATISTICAL MODELING OF ATLANTIC HURRICANE ACTIVITY USING ATMOSPHERIC REANALYSES AND IPCC SIMULATIONS AND PROJECTIONS
	Kye-Hwan Kim, Doctor of Philosophy, 2013
Directed By:	Professor Sumant Nigam, Department of Atmospheric and Oceanic Science

Atlantic hurricane activity has increased in recent decades leading to extensive investigation of its links with rising greenhouse gases (GHG). The International Panel on Climate Change (IPCC) is investigating how global-regional climate will change in the 21st century (21C) in response to GHG emissions but the deployed climate model grids are too coarse to resolve hurricanes. Projections of hurricane activity must thus be obtained, indirectly, from regional downscaling of climate using statistical and dynamical approaches; the former is adopted here.

Hurricane counts are reconstructed in 20C and projected in 21C from statistical modeling with Atlantic Sea-Surface Temperature (SST), static-stability, and zonal-wind shear as predictors. Optimal predictor definitions, including geographical domains, are identified from observational analysis (1958-2005). The viability of the statistical approach is demonstrated from the successful reconstruction of hurricane counts in both

training and independent periods, with reconstruction-observation correlations (0.72-0.86) higher than Kim and Webster's (2010; the best statistical model to date).

Statistical models for counts were also developed for each of the five analyzed IPCC- the-fifth-Assessment (AR5) models, based on their 1958-2005 simulations. The long-term trend in counts was modeled using multivariate linear regression with predictors from the ensemble-mean simulation. On the other hand, predictors from several ensemble members were used via the best subset regression technique when modeling the interannual-to-decadal count variability. Focusing on the observationally rich 1958-2005 period provided critical evaluation and a basis for selection of a credible model-subset. The 21C projections of hurricane counts by this model subset will be deemed more trustworthy than the average of all AR5-based models.

Modeling of Atlantic hurricane activity with IPCC-AR5 predictors shows a stronger count-trend in the 21C, principally, from increasing SSTs; AR5-models disagree on the trend in zonal-wind shear which is a less influential predictor in the AR5-based models compared to observations.

Decadal predictions of hurricane activity for the independent but observations-available 2006-2010 period show the promise of the best subset regression models, especially with predictors from the IPCC-Decadal (2005 ocean-initialized) experiments. According to this model, the 2013 hurricane season will be slightly more active (+1 count) but not as much as NOAA's forecast (+3 counts).

STATISTICAL MODELING OF ATLANTIC HURRICANE ACTIVITY USING ATMOSPHERIC REANALYSES AND IPCC SIMULATIONS AND PROJECTIONS

By

Kye-Hwan Kim

Dissertation submitted to the Faculty of the Graduate School of the
University of Maryland, College Park, in partial fulfillment
of the requirements for the degree of
Doctor of Philosophy
2013

Advisory Committee:
Professor Sumant Nigam, Chair
Professor Eun-Suk Seo
Professor Robert Hudson
Professor James Carton
Assistant Research Scientist Alfredo Ruiz-Barradas

Dedication

Colossians 1:15-16

"The Son is the image of the invisible God, the firstborn over all creation. For in him all things were created: things in heaven and on earth, visible and invisible, whether thrones or powers or rulers or authorities; all things have been created through him and for him. He is before all things, and in him all things hold together"

Colossians 1:9-12

"For this reason, since the day we heard about you, we have not stopped praying for you. We continually ask God to fill you through all the wisdom and understanding that the Spirit gives, so that you may live a life worthy of the Lord and please him in every way: bearing fruit in every good work, growing in the knowledge of God, being strengthened with all power according to his glorious might so that you may have great endurance and patience, and giving joyful thanks to the Father, who has qualified you to share in the inheritance of his holy people in the kingdom of light."

Acknowledgements

Above all, I am grateful to the Lord my God. “Let your glory be over all the earth.”

I would like to thank my wife Sejin for her countless devotion and support.
I am thankful to my first daughter Dahee, second daughter Dahyun, and my first and last son Daniel, for their lovely and treasurable smiles. I am so happy because finally they can take a family trip that they really wanted. I am so grateful to my father and mother for their visible and invisible love.

I am deeply grateful to my advisor, Dr. Sumant Nigam, who has been my spiritual teacher in the rest of my life. I will never forget not only his great efforts to make me a man of science, but also his incredible generosity and encouragement whenever I am down and weary.

I thank my committee members, Dr. Robert Hudson, Dr. James Carton, Dr. Alfredo Ruiz-Barradas, and Dr. Eun-Suk Seo.

I thank Dr. Eugenia Kalnay for her warm encouragement to me. She has taught me priceless wisdom in life as well as knowledge in science.

I would like to share my joyfulness with Dr. Song-You Hong, who was my master thesis advisor and mentor. I thank him for his sincere trust and encouragement during these last few years.

I thank department staff for their kind assistance. Especially, thankful to Ms. Tammy Hendershot and Mr. David Yanuk for their great administrative service and grateful help.

Thanks to my military companion, Dr. Young-Ho Cho—the numerous episodes with you in UMD would be everlastingly reminiscent in our afterlife.

Particularly, I am thankful to my valuable friends, Yan Zhou, Eric Nussbaumer, Benjamin Johnson, and Junghoon Shin for their sincere friendship and cordial encouragement.

I would like to thank my extended church family, Misung Park, Wook Yun Bae, Hyunju Moon, Hyung-Soon Park, and Hyun-Sik Jun, for their prayers and support.

I am thankful to English editor Sharon von Bergener for her valuable help and heartfelt cheer.

Financial support for this research has been provided by the support from the Republic of Korea Air Force (ROKAF)

Table of Contents

List of Tables

and the highest correlation coefficient among the designated areas for sensitivity experiment in two periods; blue is for zonal wind shear and red is for SST.

Table-3.2: Correlation coefficients and RMSE between the time series of the observed Atlantic hurricanes and the reconstruction by reanalyses; the wind shear and SST are averaged from July to October (JASO) over the periods 1981-2009 and 1958-2005.

Table-3.3: The linear trend in vertical shear of the seasonal zonal wind over KN-MDR Region of the tropical cyclones in the Atlantic basin, SST over KN-NATL in the North Atlantic basin, and reconstructed hurricanes in the period of 1958-2005. The *seasonal (JASO)* linear trend in the shear SST, and reconstructed hurricanes, noted in units of m/s/century, ºC/century, and number/century, respectively; the 95% confidence interval (CI) is noted in parenthesis. The first row documents the **observed** shear trend in recent periods (1958-2005) from reanalysis (ECMWF ERA40 and ERA-INTERIM for zonal wind shear and NOAA ERSSTv3 for SST). The second row documents the linear shear-trend in the **historical climate simulations** (1958-2005) from five IPCC-AR5 models (NCAR-CCSM4.0, GFDL-CM3.0, HadCM3.0, MPI-ESMLR, and MRI-CGCM3.0), with varying number of ensemble members (also noted), while the third row does the same for the **rcp4.5 climate projections** (2006-2100) obtained from the same models. Trends deemed statistically significant (i.e., when it passes student's t-test at 95% of significance level) are bold-faced; positive (negative) trends are in red (blue).

Table-4.1: Correlation coefficients and p-value between the time series of Sp of reanalyses and the major Atlantic Hurricanes observation; the area averaged Sp is averaged from July to October (JASO) over the periods 1958-2005. The highest

correlation coefficient and the lowest p-value are shown in red. The area and vertical level for Sp corresponding to the highest correlation are bold-faced.

Table-4.2: Correlation coefficients, p-value, and RMSE between the time series of the observed major Atlantic hurricanes and the reconstruction from reanalyses; the predictors of wind shear, SST, and Sp are averaged from July to October (JASO) over the periods 1958-2005. The highest correlation coefficient and the corresponding p-value and RMSE are shown in red. The areas for predictors of zonal-wind shear, SST, Sp corresponding to the highest correlation coefficient are bold-faced. All correlation coefficients are statistically significant at 95% significance level (p-value < 0.05).

Table-4.3: Numbers of ensemble members of each IPCC-AR5 model used in the reconstruction of all Atlantic hurricanes (AH) and major hurricanes (MH) for the period 1958-2005. Numbers of all available ensemble members for each IPCC model are bold-faced; the members used in the reconstruction of AH (blue) and MH (red). The experiment including (excluding) Sp predictor is denoted by SP (NOSP).

Table-4.4: Correlation coefficients and RMSE between the time series of the reconstruction and observed all Atlantic hurricanes (AH, the second row) and major hurricanes (MH, the third row) from three IPCC-AR5 models over the period 1958-2005. The reconstruction by using the statistical model built earlier − based on the average of ensemble members − is denoted by KN-SM$_{OLD}$; and the models developed by best subset technique is marked by KN-SM$_{NEW}$ (blue). The percentile SP effect is calculated from the correlation and RMSE values between NOSP and SP within a homogeneous statistical model for AH and MH, respectively. The extent of improvement by KN-SM$_{NEW}$ is

calculated from the correlation and RMSE values between KN-SM$_{OLD}$ and KN-SM$_{NEW}$ within a homogeneous SP option for AH and MH, respectively (red).

Table-4.5: Correlation coefficients and RMSE between the time series of the forecast from three IPCC-AR5 models and observed Atlantic hurricanes (AH, the second row and MH, the third row) over the period 2006-2010. The forecast based on RCP4.5 is denoted by RCP4.5; and based on decadal experiment is marked by DEC2005 (blue).

Table-4.6: Comparison for the number of forecasted all Atlantic hurricane counts issued by several groups' hurricane forecast model from 2002 to 2009*: Colorado State University (CSU), NOAA, NCEP's Climate Forecast System (CFS), Tropical Storm Risk (TSR), and ECMWF. To compare the performance of forecast, correlation coefficients and RMSE for each model's forecast with the observed Atlantic hurricane counts are calculated over the period. For NOAA forecast, an average of the minimum and maximum counts is used for the calculation of correlation coefficient and RMSE.

List of Figures

(a) Uz200-850 (U200 hPa-U850 hPa), (b) |Uz200-850| (|U200 hPa-U850 hPa|) are over the period 1981-2009, (c) Uz200-850 (U200 hPa-U850 hPa) over the period 1958-2005, (d) SST over the period 1981-2009, (e) SST over the period 1958-2005. All correlation coefficients are averaged from July to October over each period, and pass the significance test at 95% significance level ($p<0.05$).

* The areas are; Kim and Webster (2010) defined MDR for zonal-wind shear, MDR for SST, and the North Atlantic for SST as the area of 260ºE-320ºE and 10ºN-20ºN (hereafter, KW-MDRUz , red box in b), 280ºE-310ºE, 5ºN-15ºN (hereafter, KW-MDRSST, red box in d), 330ºE-350ºE, 35ºN-45ºN (hereafter, KW-NATLSST, green box in d), respectively. Vecchi and Sodden, 2007b defined MDR and SER for zonal-wind shear as the area of 300ºE-340ºE, 8ºN-15ºN (hereafter, VS-MDRUz, brown box in b) and 270ºE-320ºE, 13ºN-25ºN (hereafter, VS-SERUz, yellow box in b). Kim and Nigam define MDR for zonal-wind shear, MDR for SST, and the North Atlantic for SST as the area of 270ºE-300ºE, 10ºN-20ºN (hereafter, KN-MDRUz, black box in a), 270ºE-313ºE, 7ºN-16ºN (hereafter, KN-MDRSST, black box in d), and 330ºE-350ºE, 38ºN-47ºN (hereafter, KN-NATLSST, blue box in d), respectively.

Figure 3.2: The time series of the observed Atlantic hurricanes (black), the reconstructed hurricanes by KN-MDR_{Uz} and KN-$NATL_{SST}$ of reanalyses over the period 1981-2009 (red dash-dotted), by KN-MDR_{Uz} and KN-$NATL_{SST}$ over the period 1958-2005 (red solid), and by KW-MDR_{Uz} and KN-MDR_{SST} over the period 1958-2005 (blue solid) ; the correlation coefficients and RMSE value are noted in the legend.

Figure 3.3: The time series of the observed Atlantic hurricanes (black) and the reconstructed hurricanes from reanalyses of NOAA's NCEP for zonal wind shear and NOAA's ERSST V3 for SST over the period 1949-1957: the reconstruction of KN-MDR_{Uz} and the KN-$NATL_{SST}$ is shown in red and of KW-MDR_{Uz} and KN-MDR_{SST} is shown in blue; the correlation coefficients and RMSE value are noted in the legend.

Figure 3.4: The time series of the observed Atlantic hurricanes (black), reconstructed hurricanes from reanalyses, which is by KN-MDR_{Uz} and KN-$NATL_{SST}$ (red dashed) and by KW-MDR_{Uz} and KN-MDR_{SST} (blue dashed), and ensemble mean of reconstructed hurricanes from five IPCC-AR5 models (NCAR-CCSM4.0, GFDL-CM3.0, HadCM3.0, MPI-ESMLR, and MRI-CGCM3.0); the wind shear and SST are averaged over the area KN-MDR_{Uz} and KN-$NATL_{SST}$ (red solid) and KW-MDR_{Uz} and KN-MDR_{SST} (blue solid) over the period 1958-2005, respectively. The correlation coefficients and RMSE value are noted in the legend.

Figure 3.5: The spatial distribution of correlation coefficients between the observed number of Atlantic hurricane and zonal-wind shear, $Uz_{200\text{-}850}$ ($U_{200\ hPa}$-$U_{850\ hPa}$), and SST of five IPCC-AR5 models (a, f) NCAR-CCSM4.0, (b, g) GFDL-CM3.0, (c, h) HadCM3.0, (d, i) MPI-ESMLR, and (e, j) MRI-CGCM3.0. All correlation coefficients are averaged from July to October over the period 1958-2005.

Figure 3.6: The scatter plot of Uz and SST coefficients of multi-regression model from reanalyses with KN-MDRUz—KN-NATLSST (red rectangle) and KW-MDRUz—KN-MDRSST (blue rectangle) and from five IPCC-AR5 models with KN-MDRUz—KN-NATLSST (red dot) and KW-MDRUz—KN-MDRSST (blue dot) for the period 1958-

2005, respectively. The mean regression coefficients of IPCC-AR5 models are shown in circle.

Figure 3.7: The time series the Atlantic hurricanes reconstructed by KN-MDRUz and KN-NATLSST of five IPCC-AR5 models and the linear trends over the period 1958-2005. The ensemble mean of reconstructed hurricane numbers is shown in red-solid line and the corresponding linear trend and confidence interval are shown in red-dashed line in (a) CCSM4.0, (b) GFDL-CM3.0, (c) HadCM3.0, (d) MPI-ESMLR, and (e) MRI-CGCM3.0; the number of ensemble members and trend value are noted in the legend. The maximum and minimum of each model's reconstructed hurricanes are shaded in yellow and enveloped grey-solid line.

Figure 4.1: Vertical profiles of static stability parameter (Sp) averaged over the area of (a) KN-MDR SST, (b) KN-NATL SST, (c) VS-MDR Uz, and (d) VS-MDR-Wlat Uz. The 48-year (1958-2005) climatological Sp profile is shown in black; the profile of Sp averaged for the years recorded more (less) than five (two) major Atlantic hurricane counts is shown in red (blue). All areas excluding VS-MDR-Wlat are defined as in Figure 3.1; VS-MDR-Wlat is defined over the area of 300ºE-340ºE, 10ºN-20ºN.

Figure 4.2: The time series of MEI and the anomaly of observed all atlantic hurricanes for the period 1958-2005 (black-solid), the reconstruction from reanalyses (blue-solid), and three IPCC-AR5 models (red-solid); the corresponding correlation coefficients, RMSE, and linear trend values are noted in the legend. The above (below) normal MEI is displayed with pink bar (light blue bar) and the years of strong El Niño (La Niña) are denoted by red (light blue). Remarkably anomalous years corresponding to integer

hurricane number more than +4 (less than -3) are depicted in balck-dot, blue-rectangle, and red-diamond.

Figure 4.3: As in Figure 4.2 but for the time series from major Atlantic hurricanes. Remarkably anomalous years corresponding to integer hurricane number more than +3 (less than -2) are depicted in balck-dot, blue-rectangle, and red-diamond.

Figure 4.4: The difference of Atlantic hurricane counts between 5-year average for the period 2006-2010 and 48-year climatology for the period 1958-2005: for all hurricanes (a) AH SP (upper panel) and major hurricanes (b) MH SP (lower panel). Pentad prediction by the best subset regression model is from each of three IPCC models and a weighted multi-model ensemble of three IPCC models (3-IPCC MME). The counts difference corresponding to observation, reanalyses, RCP4.5, and DEC2005 is denoted with bars in black, green, red, and blue, respectively.

Chapter 1: Introduction

1.1 Background

Hurricane is the term used in the Western hemisphere for one of the general classes of strong tropical cyclones (TCs), including western Pacific typhoons and similar systems, which are known simply as cyclones in the Indian and southern Pacific Oceans (Marks 2003). Over the past two centuries, TCs have been responsible for the deaths of about 1.9 million people worldwide (Shultz et al. 2005). On average, the Gulf and east coasts of the United States suffer approximately US $5 billion (1995 US $) in cyclone damage every year (Burroughs 2007). A tropical cyclone with the maximum sustained winds of at least 64 knots (74 mph) is referred to as a hurricane in the Atlantic or East Pacific. The Saffir–Simpson scale categorizes hurricanes on a scale from 1 to 5, with 1 as the weakest and 5 as the most intense. Major hurricanes correspond to categories 3 and higher (Table 1.1).

Mark (2003) reached some general conclusions from the global distribution of tropical cyclone locations. TC formation is confined to a region between approximately 30°N and 30°S, with 87% of cyclones located within 20° of the Equator (Figure 1.1). From previous studies, some general conclusions can be drawn about the environmental conditions favorable for TC development:

- Warm sea surface temperature (SST) and large mixed-layer depth (defined as the depth of the sharp temperature inversion-thermocline between the cooler bottom

water and the warmer near surface water): Surface to 60 meter ocean temperatures above 26ºC (Gary 1979).

- Low vertical shear of the horizontal winds: High vertical wind shear inhibits tropical cyclone formation due to the detrainment of heat from the disturbance. Interference in formation due to wind shear would make it difficult for the storm's required thermal energy to become concentrated at its core (Gray 1968; Gray 1979). Vertical shear has also been shown to negatively impact cyclone genesis and growth through vertical stability (DeMaria 1996) and secondary circulation effects (Bender 1997).
- Low atmospheric static stability: Static stability is a measure of the fluid's ability to resist vertical motion when the hydrostatic equilibrium between its density structure and gravity is perturbed. A low resistance can lead to the fluid becoming turbulent (statically unstable) or laminar (statically stable) due to the effects of buoyancy only, without all other inertial effects of motion. The troposphere must be potentially unstable to sustain convection for an extended period (Marks 2003).
- High values of low-mid level tropospheric relative humidity: As dry air is entrained into convecting parcels, evaporative cooling occurs that can cause buoyancy loss. Sufficiently high levels of relative humidity would prevent such effects (Lighthill et al. 1994). Larger values of relative humidity make the tropospheric column more conductive to deep convection and enhance the surface to mid-level vertical coupling (Gray 1979).

- A large enough Coriolis parameter for large-scale rotation: The latitudinal distance from the equator is generally a minimum of 5º to allow for a sufficient Coriolis force to generate cyclonic rotation (Gray 1979; Lighthill et al. 1994). Tropical cyclones do not form within 3º of the Equator. The Coriolis parameter vanishes at the Equator and increases to extremes at the poles. Hence, a threshold value of Earth vorticity (f) must exist for a tropical cyclone to form.

In addition to the favorable conditions listed, an initial pre-existing disturbance is also necessary (Emanuel 1989; Rotunno and Emanuel 1987). Given an initial tropical disturbance with high values of concentrated vorticity, a low-level wind surge must penetrate for tropical cyclogenesis to be favorable (Gray 1998; Zehr 1992).

The presence of favorable conditions greatly depends on the large-scale flow. The conditions for tropical cyclogenesis have been found to be affected by large-scale variability such as the El Niño-Southern Oscillation (ENSO), the Atlantic Multidecadal Oscillation (AMO), the North Atlantic Oscillation (NAO), and the Atlantic Meridional Mode (AMM). Research has shown strong associations between North Atlantic TC activity, which corresponds to intensity and frequency of TC, and atmosphere-ocean variability on different timescales, including the multidecadal scale (Landsea et al. 1999). On the interannual timescale, major land-falling hurricanes increase almost threefold during La Niña events relative to El Niño events (Gray 1984; Bove et al. 1998). During El Niño seasons, upper-level winds from the west increase the wind shear over the Atlantic Main Development Region (6°–18°N, 20°–60°W; Goldenberg and Shapiro 1996), thus making conditions less favorable for both TC genesis and intensification. The potential impact of the multidecadal modes of SST variability on Atlantic TC activity

also complicates the detection of global warming signals due to the coinciding of the recent increase in Atlantic TC activity with a natural shift in the Atlantic Multidecadal Oscillation (Goldenberg et al. 2001; Kossin and Vimont 2007; Guan and Nigam 2009; Nigam and Guan 2011). Klotzbach and Gray (2008) found that during the positive phase of the AMO, approximately twice as many major hurricanes occur. The AMO is one of three interrelated Atlantic atmosphere-ocean modes with variability in the multidecadal spectrum in addition to shorter-term variations, next to the North Atlantic Oscillation and the Atlantic Meridional Mode (Marshall et al. 2001; Kossin and Vimont 2007; Grossmann and Klotzbach 2009). During the positive AMO and AMM phases, the North Atlantic warms relative to the rest of the tropics. Since potential intensity (PI) of TCs depends on the difference between local SSTs and tropical mean atmospheric temperatures (Vecchi and Soden 2007a; Swanson 2008), this localized warming causes greater PI increases than would be the case for a uniform warming of the tropics. This may explain the large magnitude of the observed recent changes in TC activity relative to the changes projected to occur with global warming (Vecchi and Soden 2007a; Swanson 2008).

1.2 Statement of the Problem and Significance

A comprehensive consensus statement on the global warming impact on TCs emerged from the World Meteorological Organization's 6th International Workshop on TCs in 2006. It stated that a firm conclusion on the existence of an anthropogenic signal in TC activity could not be drawn, but that some increase in TC intensity with global warming is likely, while changes in TC frequency (and the sign of those changes) remain

uncertain (World Meteorological Organization 2006). Working Group I of the Intergovernmental Panel on Climate Change Fourth Assessment Report (IPCC-AR4) concludes that an increase in global peak TC intensities is likely according to high-resolution models, while a global decrease in TC numbers and a possible increase in the North Atlantic is expected with medium confidence according to high and low resolution models (Meehl et al. 2007; their Table 11.2).

As to the cause of the increase in Atlantic TC activity, there are intense debates in context of climate change. Some studies (e.g., Goldenberg et al. 2001; Zhang and Delworth 2006, Nigam and Guan 2011) suggest that increased TC activity is related to the natural variability of Atlantic sea surface temperatures (SSTs), especially the Atlantic Multidecadal Oscillation (AMO; Enfield et al. 2001; Delworth and Mann 2000; Guan and Nigam 2009), while others attribute the increase in activity to anthropogenic climate change (Webster et al. 2005; Trenberth and Shea 2006; Mann and Emanuel 2006; Holland and Webster 2007). The attribution of heightened TC activity to natural variations and/or secular change of climate thus remains challenging, especially in view of the short length of the observational record and its uneven quality (Landsea 2007; Mann et al. 2007; Chang and Guo 2007; Vecchi and Knutson 2008; Landsea et al. 2010), and the modest simulation skill of current climate models; leaving much to debate.

There is extensive discussion of the role of the North Atlantic SST in driving TC activity in previous studies (Landsea et al. 1999; Zhang and Delworth, 2006; Trenberth and Shea, 2006). More than half of the decadal time-scale variance in the annual Atlantic TC count can be explained by SST variations in the main development region (MDR; Mann and Emanuel 2006). The nonlocal SSTs, i.e., the ones outside the MDR, are also

influential as indicated by analyses that show the MDR SST variations relative to the global tropical average to be more pertinent (Emanuel 2005; Swanson 2008;Vecchi et al. 2008; Vecchi and Soden 2007; Nigam and Guan 2011), and studies that document the impact of the Pacific SST on tropospheric circulation (vertical shear and stability) over the tropical-subtropical Atlantic (e.g., Elsner et al. 2001; Aiyyer and Thorncroft 2006; Camargo et al. 2007; Nigam and Guan 2011).

A number of studies have indicated that vertical shear of the horizontal (zonal) wind over the tropical Atlantic is a notably influential environmental variable, impacting tropical cyclone activity (Gray 1968; DeMaria 1996; Goldenberg et al. 2001; Camargo et al. 2007). Large vertical shear is detrimental to cyclone formation (Pielke and Landsea, 1999; Goldenberg et al., 2001; Emanuel and Nolan, 2004; Camargo et al., 2007) as well as intensification (Zehr, 1992; DeMaria, 1996; Frank and Ritchie, 2001). Wind shear acts to disturb the structure of the TC, making the TC more susceptible to other interferences and less efficient at using ocean heat. During El Niño seasons, upper-level winds from the west increase wind shear over the Atlantic MDR (Goldenberg and Shapiro 1996), thus making conditions less favorable for both TC genesis and intensification. In a warmer climate, shear may increase in the Atlantic and East Pacific and decrease in the West Pacific (Vecchi and Soden 2007b, Nigam and Guan 2011).

The above discussion highlights the challenges in detection of a possible climate change signal in the Atlantic TC activity from the background noise generated by interannual-to-multidecadal natural variability. The challenge is compounded by the short length of the observational records vis-à-vis the multidecadal variability timescales, and by the inability of the current class (IPCC-AR5) of climate system models to simulate the

large-scale structure of 20th century climate variability and change, let alone the tropical cyclone structure and distributions. The 21st century projections and decadal predictions of TC activity are likewise hindered by the uncertainties in evolution of multidecadal natural variability in the Atlantic and Pacific basins, and the related and unrelated changes in regional climate and the large scale environment, and by the model-resolution limitation imposed by the current-day computational infrastructure.

1.3 Motivation and Scientific Questions

Several recent modeling studies and related analyses project a reduction in TC activity in the 21st century, based largely on the significantly increased wind-shear over MDR in the IPCC-AR4 projections (Garner et al., 2009; Vecchi and Soden, 2007b; Gualdi et al., 2008; Bengtsson et al., 2007; Zhao et al., 2009). Vecchi and Soden (2007b) projected a 10% increase in wind shear over the Caribbean for each degree of global warming, from analysis of an 18-member multi-model ensemble of 21st century IPCC-AR4 projections (SRES A1B scenario). Garner et al. (2009) also stated that vertical wind-shear was the main driver in the projected reduction of TC activity. However, many of these studies analyze only the IPCC 21st century projections, and not the 20th century simulations that can provide a reading on the projecting models' performance.

Although popular, multi-model assessments of the change in Atlantic TC activity in IPCC-AR4 climate projections (e.g., Vecchi and Soden, 2007) are developed generally without consideration of the projecting models' simulation potential; not factoring for the model performance can skew multi-model based assessment. Note, the model performance can be evaluated as the same AR4 coupled models were also used to

simulate the climate of the 20th century, a period for which validating observational/reanalysis records exist; for instance, the simulation of the zonal-wind shear trend can be assessed.

Not only that, the IPCC simulations of 20th century climate are generally challenged in the simulation of regional circulation and hydroclimate features over both continental (Ruiz-Barradas and Nigam 2010) and oceanic regions (e.g., Kavvada et al. 2013). Unfortunately, it is the regional features, such as zonal wind shear over the tropical western-central Atlantic and SST over the Main Development Region in the tropical Atlantic, that emerge as key statistical predictors of the Atlantic TC counts in observational analyses. As such, directly using the variations in these features to infer changes in Atlantic TC activity (e.g., as through multi-model ensemble based composites) is potentially problematic. At a minimum, there is need to re-weigh the importance of the key predictors in context of the IPCC simulations; we refrain from choosing new predictors, in the interest of keeping the statistical model rooted in physicality.

This research is motivated by the need to use the IPCC-AR4 and AR5 simulations and projections as effectively as possible to infer the changes in Atlantic TC activity in both the near-term (i.e., decadal) and long-term (i.e., centennial) climate projections. As noted before, the AR5 model resolution remains too coarse to resolve tropical cyclone, especially in the incipient stage, and dynamic downscaling remains prohibitively expensive, computationally, on account of long integrations and several ensemble members. Statistical models are thus an important tool in the interim for drawing inference regarding potential changes in cyclone activity.

From this point of view, the undertaken study seeks to address the following scientific questions:

- *Is there compelling evidence from observational analyses and climate modeling experiments for increasing vertical wind shear (i.e., ∂U/∂z) over the tropical Atlantic with increasing greenhouse warming of the planet? Is there a secular increase in shear manifest in the 20th century observational record? Do the IPCC-AR4 and AR5 climate system models indicate an unequivocal shear increase? Shouldn't wind shear projections for the 21st century be weighted by the skill of the same models in simulating 20th century wind shear variability?*
- *What is the relative significance of vertical wind shear, SSTs (local and remote), and regional atmospheric static stability in influencing Atlantic TC counts? Which – SSTs or vertical wind shear – is more influential? Is the significance of the three factors in the IPCC climate simulations similar to that manifest in the 20th century observations?*
- *Can the Atlantic TC counts be statistically reconstructed using observed vertical wind shear, SSTs, and atmospheric static stability? How effectively can TC counts be reconstructed using IPCC AR4 and AR5 simulations of 20th century climate?*
- *Is the optimal reconstruction of TC counts with the IPCC simulation datasets obtained from the ensemble-mean simulation or from use of multiple ensemble members of a given model?*
- *What is the efficacy of the statistical reconstruction model in the hindcast prediction of TC counts, i.e., in an earlier period that is independent of the model*

training period, but one for which validating TC count observations exists? Does the hindcast prediction skill of the statistical model vary among IPCC-AR5 simulations, and between observations and these simulations?

- *Finally, what inference can be drawn from the statistical model regarding changes in Atlantic TC activity in both the near-term (i.e., decadal) and long-term (i.e., centennial) climate projections? How does this guidance compare with that obtained from dynamical downscaling and other related analyses?*

1.4 Objectives

The thesis objective is to systematically seek answers to the above questions, from statistical downscaling, while drawing on our knowledge of climate dynamics to gain insights into the obtained findings. The major goals of this work are to:

- Investigate and characterize the change in environmental factors such as wind shear, SST, and static stability in the 20th and 21st centuries;
- Advance our understanding of the influence of these environmental factors on Atlantic hurricane activity, especially under a warming climate;
- Develop a statistical model to reconstruct and predict Atlantic TC counts based on the Atlantic wind shear, SST, and static stability. The model will be developed separately for the observed (reanalysis) and simulated 20th century SST, circulation, and temperature records
- Use the model to infer the change in Atlantic hurricane activity in the 21st century and the predictability of Atlantic hurricane activity in the near future.

1.5 Thesis Outline

An observational analysis of the change in Atlantic wind shear in various reanalyses of 20th century atmospheric circulation, and the linear trend in vertical wind-shear over the tropical Atlantic in both 20th century climate simulations and 21st century climate projections (SRES A1B scenario) of five IPCC-AR4 models are analyzed in Chapter 2. In Chapter 3, the analysis is extended to the role of wind shear and SST on the change of Atlantic hurricane counts, as well as to critically examine and discuss the change of the Atlantic hurricane counts in 21st century prediction through statistical modeling based on IPCC-AR5. Chapter 4 presents the predictability of Atlantic hurricane activity through statistical modeling based on wind shear, SST, and static stability of IPCC-AR5 simulations and projections as dynamic and thermodynamic variables. Finally, the summary and concluding remarks follow in Chapter 5.

1.6 Tables

Table-1.1: Saffir–Simpson scale of hurricane intensity is available at the web site of (http://www.aoml.noaa.gov/hrd/tcfaq/D1.html).

Category	Maximum sustained wind speed		
	mph	ms^{-1}	kts
1	74-95	33-42	64-82
2	96-110	43-49	83-95
3 (Major)	111-129	50-58	96-112
4 (Major)	130-156	59-69	113-136
5 (Major)	≥157	≥70	≥137

1.7 Figures

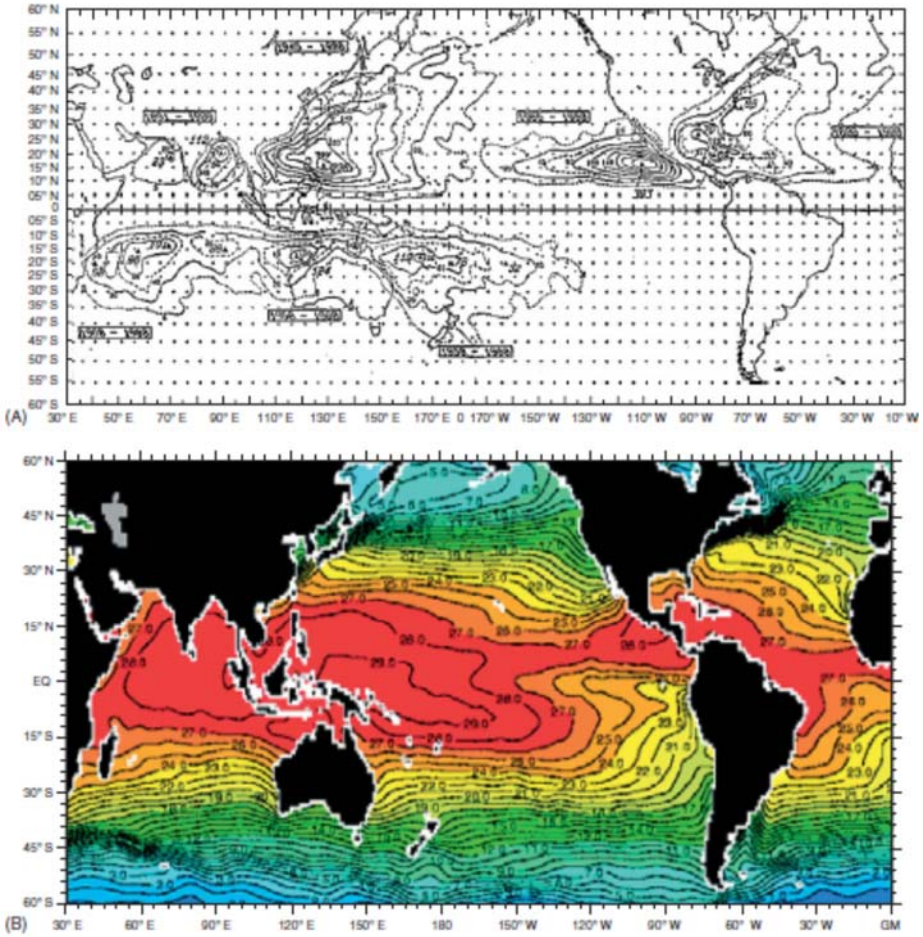

Figure 1.1: (a) Counts of tropical cyclones per 100 years within 140km of any point. Solid triangles indicate maxima, with values shown. Period of record is shown in boxes for each basin. (b) Annual sea surface temperature distribution (°C) (Marks 2003).

Chapter 2: The Change of Tropical Atlantic Wind Shear in IPCC-AR4 Projections

2.1 Introduction

Climate model integrations undertaken for the Intergovernmental Panel on Climate Change 4th Assessment Report (IPCC-AR4) project changes in tropical cyclone (TC) activity in a warmer climate, indirectly, through SST-change in the cyclone development region of the tropical Atlantic (thermodynamic control) and vertical wind-shear change over the same region (environment control); the coarse model resolutions do not permit direct projections of cyclone activity.

Vertical shear of the horizontal (zonal) wind over the tropical Atlantic is widely viewed as an influential environmental variable, impacting both cyclone intensity and frequency. Large vertical shear is detrimental to cyclone formation (Pielke and Landsea, 1999; Goldenberg et al., 2001; Emanuel and Nolan, 2004; Camargo et al., 2007) as well as intensification (Zehr, 1992; DeMaria, 1996; Frank and Ritchie, 2001). Saunders and Lea (2008) claimed that wind shear explains more variance in Atlantic TC activity than SST in the 1965-2005 period.

Nigam and Guan (2011) find the increased westerly wind shear related with the secular but non-uniform warming of the oceans (including tropical Atlantic) important in limiting the impact of ocean warming on Atlantic TC activity in their 20th century observational analysis; the dynamical (shear-related) impact offsetting the thermodynamic (SST-related) one. These authors also show Pacific decadal SST

variability to be influential on Atlantic TC counts, in part, through vertical wind shear variations over the main development region (MDR; Mann and Emanuel 2006 6°–18°N, 20°–60°W) of the tropical Atlantic.

Recent modeling studies suggest that Atlantic TC frequency could decrease as the climate warms (Garner et al., 2009; Vecchi and Soden, 2007b; Gualdi et al., 2008; Bengtsson et al., 2007; Zhao et al., 2009). The decrease is mostly attributed to the increased wind shear over MDR. Vecchi and Soden (2007b) project a 10% increase in wind shear over the Caribbean for each degree of global warming, from analysis of an 18-member multi-model ensemble of 21st century IPCC-AR4 projections (SRES A1B scenario). Garner et al. (2009) also found vertical wind-shear to be the main driver in the projected reduction of TC activity.

Although popular, multi-model assessments of the change in Atlantic TC activity in IPCC-AR4 climate projections are developed generally without consideration of the projecting models' simulation potential (e.g., Vecchi and Soden, 2007); not factoring for the model performance can skew the multi-model based assessment. Note, model performance can be evaluated as the same AR4 coupled models were also used to simulate the climate of the 20th century, a period for which validating observational/reanalysis records exist; for instance, simulations of the vertical wind shear trend can be assessed, as here.

This chapter focuses on a widely analyzed subset of IPCC-AR4 simulations and projections, analyzing all available ensemble members for each model. A performance context (20th century wind shear simulation) for each model is provided when discussing its projection of vertical wind shear over the tropical Atlantic. Data sets and the analysis

technique are briefly discussed in section 2.2, model performance in section 2.3, and model projections in section 2.4.

2.2 Data and Methodology

Monthly-mean zonal and meridional winds at the 150 hPa and 700 hPa vertical levels were obtained from the European Centre for Medium-Range Weather Forecasts (ECMWF) 40-Year Re-Analysis dataset (ERA-40; 1958-2001; Uppala et al. 2005;), NOAA's NCEP Reanalysis (1949-onwards; Kalnay et al., 1996), and NOAA's 20th Century Reanalysis (20CR; 1891-2008; Compo et al., 2011). The 20CR dataset was developed from short-term forecasts generated from assimilation of synoptic surface/sea-level pressure and monthly SST and sea-ice boundary conditions.

The linear trend in vertical wind-shear was analyzed in five IPCC-AR4 20th century simulations and 21st century projections (with SRES A1B scenario); the gridded monthly-averaged data was downloaded from the Program for Climate Model Diagnosis and Intercomparison. The analyzed models are from the US National Center for Atmospheric Research (NCAR-CCSM3.0), NOAA's Geophysical Fluid Dynamics Laboratory (GFDL-CM2.1), U.K. Meteorological Office's Hadley Center (HadCM3.0), Japan's Meteorological Research Institute (MRI-CGCM2.3.2a), and Germany's Max Planck Institute (ECHAM5).

The vertical wind shear was defined as the magnitude of the vector difference of the monthly 150 and 700 hPa winds (=$\left|\vec{V}_{150\,\mathrm{hPa}} - \vec{V}_{700\,\mathrm{hPa}}\right|$). These levels were chosen instead of the commonly used 200 and 850 hPa levels (e.g., Goldenberg et al., 2001;

Zhang and Delworth 2006; Vecchi and Soden 2007b) following Vecchi and Soden's recommendation. The choice is apt as seen later from the displayed vertical wind structure (Figs. 2.1b-d and 2.2).

2.3 Changes of Tropical Atlantic Wind Shear in IPCC-AR4

2.3.1 Atmospheric reanalyses

The vertical wind-shear trend is evaluated across two 20th century periods: For the first (1949-2008), In this recent 60-year period reanalysis from NOAA's 20CR and NCEP, the shear trend is +6.53 and +8.73 m/s/century, respectively, yielding a mean trend of +7.63 and standard deviation (SD) of ±1.10 m/s/century, as indicated in Table-2.1. The individual trends in zonal and meridional wind shear, also listed in the Table, show the former to be dominant. For the second period (1958-2001), three reanalysis-based estimates are available: +7.15 (20CR), +14.65 (NCEP), and +8.77 m/s/century (ERA-40); yielding a mean trend of +10.19 and SD of ±3.22 m/s/century.

Zonal-wind shear, which again dominates wind-shear trends, is displayed in Fig. 2.1a. In the second-half of the 20th century, all three reanalyses show positive trend up to 1980s and a negative one since, albeit with varying magnitude. The decreasing shear in recent decades is consistent with the pronounced increase in Atlantic TC activity in the same period (Kossin et al., 2007; Emanuel, 2005a; Emanuel, 2007; Holland and Webster, 2007; Wu and Wang, 2008; Nigam and Guan 2011). The variation of zonal wind-shear across the full 20th century (from NOAA's 20CR reanalysis) is also shown in Fig. 2.1a, for context; the 1901-2008 period trend (blue dashed line) is slightly negative (−0.24

m/s/century), i.e., very different from the steep positive trend in the latter part of the century (+6.53 m/s/century).

The vertical profile of the fall-season (June to October: JASO) zonal wind (and its linear trend), averaged over MDR, is shown in Figs. 2.1b-d to assess the relative role of the upper and lower troposphere in generation of the zonal-wind shear trend. As apparent, the shear trend arises, largely, from the upper-level where zonal wind and its trend are both positive.

2.3.2 IPCC-AR4 Simulations of 20th Century

The vertical wind-shear trend in IPCC-AR4 simulations of 20th century (1901-1999) climate are noted in Table-2.1. The ensemble-mean trend is positive and statistically significant in 2 of the 5 model simulations: GFDL-CM2.1 (+1.16 ±0.45 m/s/century based on a 3-member ensemble) and HadCM3.0 (+0.65 ±0.21 m/s/century based on 2-member ensemble); zonal wind shear dominates the trend, as in observations. In the other simulations (CCSM3.0, ECHAM5, and MRI-CGCM), the SD of the intra-ensemble trends is 2-3 times larger than the ensemble-mean, leading to statistically insignificant wind-shear trends.

The ensemble-mean vertical profile of the MDR-averaged fall zonal wind (and related linear trend) is shown for three 20th century simulations in Figs. 2.2a-c. In both GFDL-CM2.1 and HadCM3.0, upper-levels exhibit larger trends, as in observations; only the GFDL profile exhibits a negative trend (albeit weak) at the lower level, like observations (Figs. 2.1b-d). The HadCM3.0 profile is essentially unchanged at lower-levels while the CCSM3.0 one is likewise at all levels.

Based on similar sign of the statistically-significant vertical wind-shear trend and the similar vertical profile of zonal-wind trends in the GFDL-CM2.1 and HadCM3.0 20th century simulations *and* corresponding observations/reanalyses, these two models are, to an extent, deemed credible in their 21st century projections of these quantities; our working hypothesis.

2.3.3 IPCC-AR4 projections of 21th Century

Several recent modeling studies (and related analysis) project a reduction in TC activity in the 21st century, based largely on the significantly increased wind-shear over MDR in the IPCC-AR4 projections (Garner et al., 2009; Vecchi and Soden, 2007b; Gualdi et al., 2008; Bengtsson et al., 2007; Zhao et al., 2009). As noted earlier, many of these studies analyze only the IPCC 21st century projections, and not 20th century simulations that can provide a reading on model performance. Table-2.1 shows the 21st century vertical wind-shear trends from all 5 model projections, using all publicly available ensemble members.

The fall wind-shear trend is *negative* in 3 of the 5 projections: −2.42 ±0.36 (CCSM3.0); −0.40 ±0.55 (GFDL-CM2.1); and −0.05 ± 1.11 m/s/century (MRI-CGCM). The trend is however statistically significant only in CCSM 3.0 where SD of the intra-ensemble trends is smaller than the ensemble-mean; not so, in the other two. The GFDL trend can be viewed as marginally significant as the zonal and meridional wind-shear trends are, individually, significant by the above measure (cf. Table-2.1).[1] In contrast, the trend is *positive* and statistically significant in the ECHAM5 projections (+1.67 ±0.95

[1]And because 2 of the 3 ensemble members exhibit negative wind-shear trends (−1.11,−0.30), like the ensemble-mean (−0.40 m/s/century) which, of course, did not clear the significance test, as noted above.

m/s/century). HadCM3.0 exhibits a much stronger positive trend (+7.69 m/s/century) but its statistical significance cannot be assessed on account of its 1-member ensemble.

If 21st century shear trend projections are weighted by 20th century model performance (from simulation-observation intercomparison), only two projections stand out: GFDL-CM2.1 and HadCM3.0. The CM2.1 projects a negative *zonal*-shear tendency (−0.99 ±0.84 m/s/century) based on a 3-member ensemble, while the 1-member HadCM3.0 ensemble projects a positive tendency (+7.67 m/s/century); the ensemble-mean, fall-season MDR zonal wind profiles (and related linear trend) are shown in Figs. 2.2d-f.

Given the discord, one can only conclude that there is no unequivocal evidence from the analyzed IPCC model projections for increasing wind-shear over MDR! As such, this analysis questions the widely reported findings based on indiscriminate multi-model averaging; weighting all model projections equally may find resonance in ideals of the body politic, but a rational basis is needed for its practice in scientific analysis.

2.4 Summary and Conclusions

The evidence for a statistically-significant *negative* trend in MDR's *zonal* wind-shear in IPCC-AR4's 21st century projections comes from 2 of the 5 analyzed climate projections. Only one of the 2 projecting models (GFDL-CM2.1) however passed our rudimentary model-performance check. As such this evidence must be considered preliminary. The other model that cleared the performance check (HadCM3), on the other hand, projects a *positive* wind-shear trend but its statistical significance remains to be ascertained. Regardless of the significance outcome, a compelling case for an increasing

vertical wind-shear over MDR cannot be made from analysis of the five leading IPCC-AR4 simulations and projections – in contrast with reported claims based on indiscriminate multi-model averaging.

Should analysis of additional AR4 (and soon-to-be-available AR5) simulations and projections indicate negative wind-shear trends over MDR, it would dampen prospects of a dynamical offset of the effects of anthropogenic SST warming on Atlantic hurricane activity. Negative wind-shear trend should, in fact, exacerbate the thermodynamic influence of rising SSTs on the hurricane activity. An analysis of the simulated and projected SSTs is underway.

2.5 Tables

Table-2.1: The linear trend in vertical shear of the seasonal zonal, meridional, and vector wind over the Main Development Region (6°–18°N, 20°60°W) of the tropical cyclones in the Atlantic basin. The *fall* linear trend in (u_{150}–u_{700}), (v_{150}–v_{700}), and $\left|\vec{V}_{150} - \vec{V}_{700}\right|$ is noted in units of m/s/century; the standard deviation (SD) is noted in parenthesis when multiple estimates are available. The first row documents the **observed** shear trend in two recent periods (1949-2008, 1958-2001) from atmospheric reanalysis (NOAA 20CR, NOAA NCEP, ECMWF ERA40); the mean trend and related SD are noted when more than one reanalysis estimate is available. The second row documents the linear shear-trend in the **20th century climate simulations** (1901-1999) from five IPCC AR4 models (NCAR-CCSM3.0, GFDL-CM2.1, HADCM3.0, ECHAM5, and MRI-CGCM2.3.2a), with varying number of ensemble members (also noted), while the third row does the same for the **21st century climate projections** (2001-2099) obtained from the same models. Trends deemed statistically significant (i.e., when ensemble-mean is larger than SD) are bold-faced; positive trends are in red. The result from Vecchi and Soden's (2007) analysis of 21st century projections is noted in the bottom sub-row, for context.

Atmospheric Reanalyses			**1949-2008**		**1958-2001**		
			NOAA 20CR	**NOAA NCEP**	**NOAA 20CR**	**NOAA NCEP**	**ERA40**
		u(SD)	6.53	9.38	7.00	15.48	9.64
		v(SD)	-1.65	-1.05	-2.30	-4.11	-2.60
		$\|\vec{V}\|$(SD)	6.53	8.73	7.15	14.65	8.77
			Mean		Mean		
		u(SD)	**7.95**(±1.43)		**10.71**(±3.55)		
		v(SD)	**-1.35**(±0.30)		**-3.00**(±0.80)		
		$\|\vec{V}\|$(SD)	**7.63**(±1.10)		**10.19**(±3.22)		
			NCAR-CCSM3.0	**GFDL-CM2.1**	**HADCM3.0**	**ECHAM5**	**MRI-CGCM2.3.2a**
20C (1901-1999)	**IPCC AR4 models**	# of Ensemble members	7	3	2	4	5
		u(SD)	-0.17(±0.82)	**1.14**(±0.53)	**0.64**(±0.21)	0.21(±0.56)	0.27(±0.71)
		v(SD)	0.11(±0.19)	**0.21**(±0.01)	**0.25**(±0.01)	0.13(±0.21)	0.18(±0.28)
		$\|\vec{V}\|$(SD)	-0.17(±0.82)	**1.16**(±0.45)	**0.65**(±0.21)	0.15(±0.52)	0.27(±0.69)
21C (2001-2099)	**IPCC AR4 models**	# of Ensemble members	7	3	1	4	5
		u(SD)	**-2.45** (±0.37)	**-0.99**(±0.84)	7.67	**1.70**(±1.03)	-0.06(±1.16)
		v(SD)	**0.51**(±0.27)	**-0.39**(±0.26)	-0.35	**0.35**(±0.16)	0.49(±0.23)
		$\|\vec{V}\|$(SD)	**-2.42**(±0.36)	-0.40(±0.55)	7.69	**1.67**(±0.95)	-0.05(±1.11)
	Vecchi and Soden (2007b)		**Significant increase**				

2.6 Figures

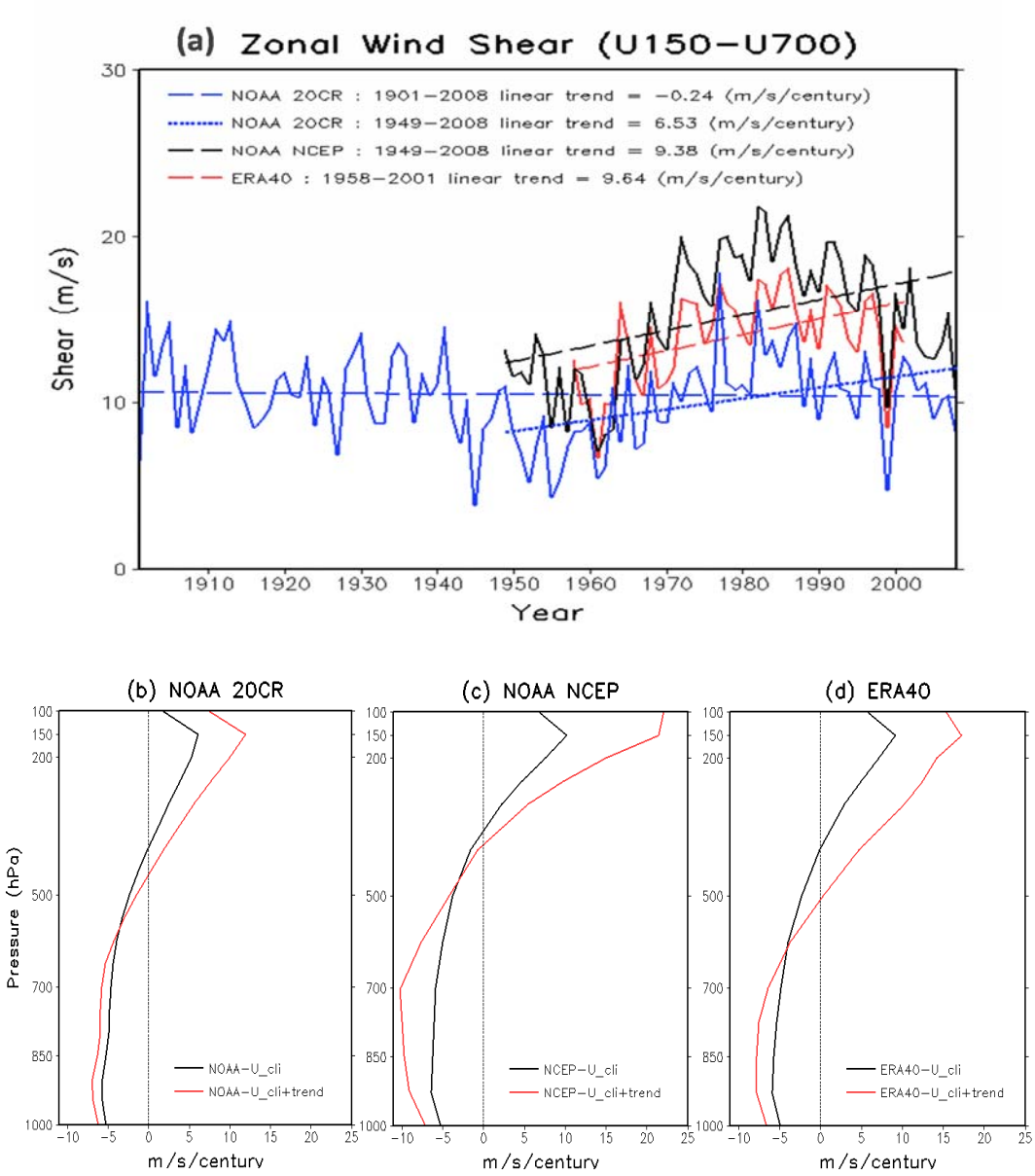

Figure 2.1: (a) Fall-season zonal wind shear ($u_{150hPa} - u_{700hPa}$) over the Main Development Region of the tropical cyclones in the Atlantic basin in three atmospheric reanalyses: NOAA 20CR (1901-2008, blue); NOAA NCEP (1949-2008, black); and ECMWF ERA40 (1958-2001, red). Colored dashed lines depict the linear trend in zonal wind shear; the trend period and value is noted in the legend. For NOAA 20CR, the trend is computed for the full period as well as the NCEP reanalysis period (1949-2008). **(b)-(d)** Vertical profiles of the MDR-averaged zonal wind (and linear trend) are intercompared in the common reanalysis period (1958-2001): The 44-year climatological fall-season profile is shown in black; the corresponding profile with the linear trend (over the 44-year period) applied for a century is shown in red; a century-long application was used to highlight the trend structure.

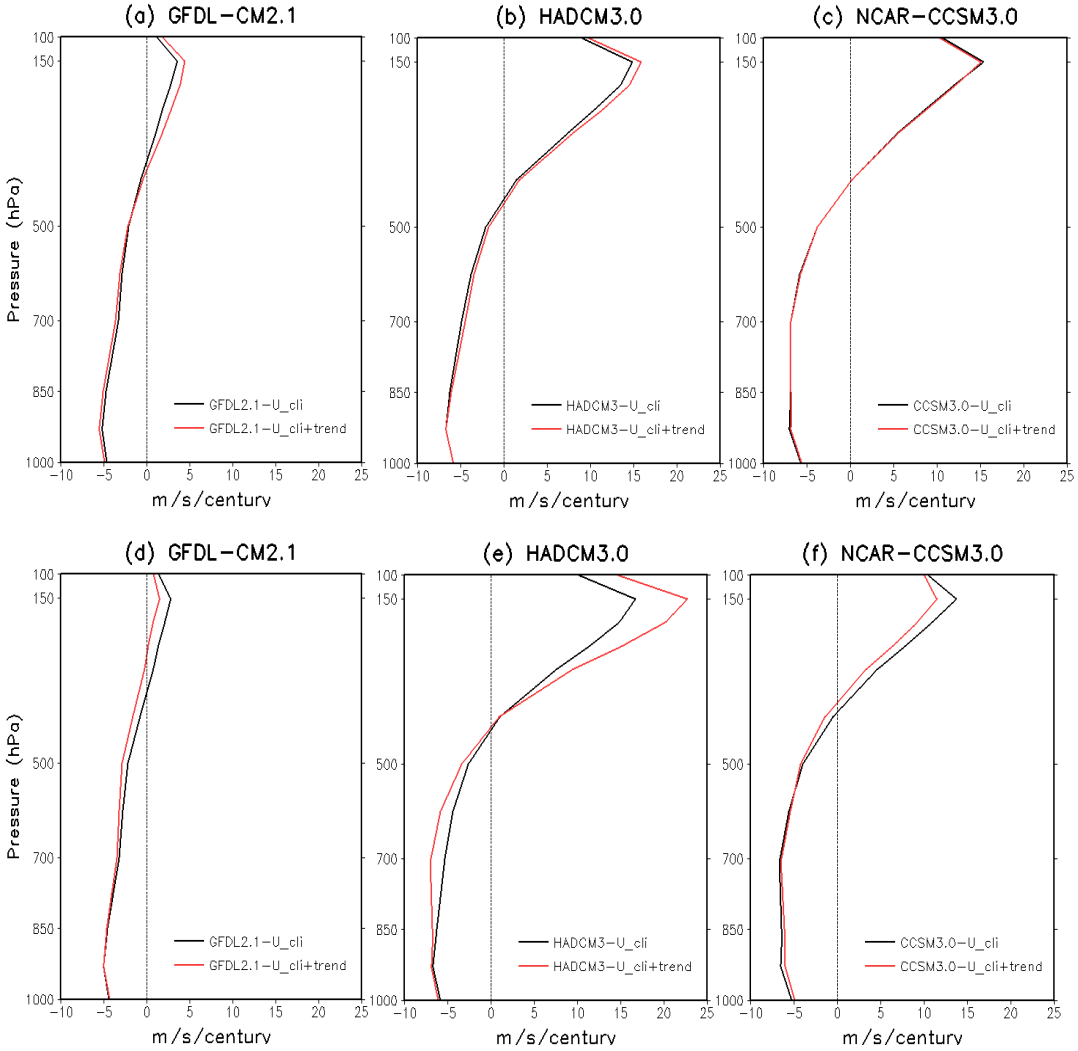

Figure 2.2: As in Figure 1 but for ensemble-mean profiles from the IPCC AR4 20th Century climate simulations (1901-1999; upper panels, *a-c*) and 21st century climate projections (2001-2099; lower panels, *d-f*). Results from three commonly analyzed models are shown in both cases: GFDL-CM2.1 (*a,d*); HADCM3.0 (*b,d*); and NCAR-CCSM3.0 (*c,f*).

Chapter 3: Statistical Modeling of Atlantic Hurricane Counts from Wind Shear and SST Variations in 20th Century Observations, and the IPCC-AR5 Simulations and Projections

3.1 Introduction

In statistical modeling of the Atlantic tropical cyclone (or TC) counts, the tropical Pacific and Atlantic SSTs as well as the vertical shear of the horizontal wind over the tropical Atlantic basin are key predictors (e.g., Kim and Webster 2010), representing the combined effects of large-scale and regional dynamics, and local thermodynamics. This chapter focuses on the observational record for the second half of the 20th century, the IPCC-AR5 climate simulations for the 20th century, and the IPCC-AR5 climate projections for the 21st century. The simulations and projections from the five leading IPCC-AR5 climate system models (NCAR-CCSM4.0, GFDL-CM3.0, HadCM3.0, MPI-ESMLR, and MRI-CGCM3.0) are analyzed, including all available ensemble members from each model. As the horizontal resolution of these models is too coarse for capturing tropical cyclone development, any inference about the changing statistics of tropical cyclone counts and/or intensity can only be drawn by statistical and/or dynamical downscaling of the century-long climate simulations and projections.

Dynamical downscaling can yield improved simulation and projection of *regional* circulation and hydroclimate from the higher-resolution representation of physical (orography, coastlines, vegetation, lakes, etc.) and dynamical (fronts, meso-scale convective complexes or MCS) features, and their interaction with the imposed large-

scale horizontal flow at the lateral boundaries of the region. But these models are, computationally, no less burdensome, especially in context of downscaling the century-long IPCC-AR5 simulations and projections from multiple models, each with several ensemble members. The benefits of dynamical downscaling are moreover, seldom, fully realized as the prism being used is still a complex weather forecasting model with numerous parameterizations of physical processes.

An alternate to dynamical downscaling is statistical downscaling of regional circulation and hydroclimate. The goal is still the same – a more contextual representation of regional flow and precipitation, consistent with the regional terrain, land-surface types, coastlines, and other physical attributes of the lower boundary – but with the methodology used in connecting the larger-scale flow variations to regional climate circumventing the complex weather forecasting models. The larger-to-regional scale links are instead provided by a statistical model that is developed using existing observations. An important premise of this approach is that the observational record used in statistical model development be 'rich' in spatiotemporal complexity so that the obtained statistical model remains relevant with independent data (in observations and IPCC-AR5 simulations and projections).

Multivariate linear regression models for the Atlantic tropical cyclone counts are developed in this chapter using the zonal-wind shear and Atlantic SST as predictors. Optimal predictors (e.g., the spatial domain used for defining the zonal-wind shear anomalies) were first selected based on extensive univariate correlation analysis of the observed Atlantic TC counts with atmospheric observations (reanalysis data). A multivariate linear regression model for TC counts was then developed, separately, for

the second-half of the 20th century climate observations and climate model simulations. The reconstruction of TC counts with the statistical models in the training period provides a baseline evaluation of the models' performance, and an assessment of the relative roles of zonal-wind shear and SST anomalies in influencing TC counts in the observed and simulated climates. Such benchmarking would seem important when using these statistical models to infer changes in TC counts in 21st century climate projections.

The data sets and the analysis technique are briefly discussed in section 3.2; the statistical modeling of Atlantic hurricane counts using wind-shear and SST observations in section 3.3; the reconstruction of hurricane counts from the IPCC-AR5 model simulations of wind-shear and SST in section 3.4; and the projection of hurricane counts from the IPCC-AR5 model projections of regional wind-shear and SST in section 3.5.

3.2 Data sets and Methodology

Monthly-mean zonal winds at the 200 hPa and 850 hPa vertical levels were obtained from the European Centre for Medium-Range Weather Forecasts (ECMWF) Re-Analysis dataset (ERA-40; Uppala et al. 2005) for a 41-year (1958-1988) period, ERA interim (Berrisford et al., 2009) for a 21-year (1989-2009) period, and NOAA's NCEP Reanalysis (Kalnay et al., 1996) for a 9-year (1949-1957) period. Monthly-mean Sea Surface Temperature (SST) was from the Extended Reconstructed Sea Surface Temperature Version 3 (ERSSTv3; Smith et al., 2008) for a 61-year (1949-2009) period. The hurricane data for Saffir-Simpson category storms 1 to 5 for a 61-year (1949-2009) period was downloaded from the NOAA Hurricane Best Track Database.

The wind shear, SST, and the Atlantic hurricane counts were analyzed in five IPCC-AR5 20th century simulations (i.e., climate system model integrations for the 20th century with the observed time-dependent greenhouse gas concentrations) and 21st century projections with a medium mitigation scenario of Representative Concentration Pathway 4.5 (RCP4.5), where carbon dioxide concentrations stabilize at 650 ppmv near the year 2100, but eventually reach a value of 1350 ppmv. The gridded monthly-averaged data was downloaded from the Program for Climate Model Diagnosis and Intercomparison. The analyzed models are from the US National Center for Atmospheric Research (NCAR-CCSM4.0), NOAA's Geophysical Fluid Dynamics Laboratory (GFDL-CM3.0), U.K. Meteorological Office's Hadley Center (HadCM3.0), Germany's Max Planck Institute (MPI-ESMLR), and Japan's Meteorological Research Institute (MRI-CGCM3.0).

The vertical wind shear was defined as the difference of the monthly 200 and 850 hPa winds (=$U_{200\ hPa}-U_{850\ hPa}$) following the commonly used levels (Goldenberg et al., 2001; Zhang and Delworth 2006; Vecchi and Soden 2007b) and compared with the vertical wind shear defined using the adjacent 150 hPa and 700 hPa levels ($U_{150\ hPa}-U_{700\ hPa}$), and also with the *magnitude* of the vertical wind shear of the difference of 200 and 850 hPa winds ($|U_{200\ hPa}-U_{850\ hPa}|$).

Statistical analysis was used to select the best predictor regions for Atlantic wind shear and SST, using correlations with Atlantic hurricane counts as the metric. The robustness of the linear trend in wind shear, SST, and reconstructed hurricane counts (from a multi-linear regression model) was assessed using the student's t-test at 95% significance level.

3.3 Statistical Modeling of Atlantic hurricane counts from wind-shear and SST observations

Statistical modeling of Atlantic hurricane activity is based on three representative methods: the first uses empirical relationships between observed hurricane activity and the vertical wind-shear (related to large scale atmospheric dynamics) and SST (related to oceanic thermodynamics) variations; the second downscales dynamical information from a climate system model using a high resolution regional climate model; while the third uses both of the above approaches. For instance, to forecast hurricane activity, Klotzbach (2007) uses indices of the ENSO phase, SST over the east Atlantic, and of sea level pressure (SLP) over the tropical Atlantic along with statistics of the storms in the prior season to issue an outlook forecast for hurricanes. On the other hand, Vitart et al. (2007) utilized dynamical information from coupled ocean-atmosphere climate models directly for seasonal hurricane prediction. In contrast, Kim and Webster (2010) developed a hybrid forecast model for seasonal hurricane activity in the North Atlantic, based on a dynamical coupled ocean-atmosphere model forecast of seasonal circulation (wind-shear specifically) and empirical prediction models.

3.3.1 Sensitivity experiment

Kim and Webster (2010) identified zonal-wind shear in the Main Development Region (MDR; 260ºE-320ºE,10ºN-20ºN) of the tropical Atlantic (referred as KW-MDR_{Uz}), and SSTs in the North Atlantic basin (referred as KW-$NATL_{SST}$) as optimal predictors of hurricane activity. The authors showed that additional consideration of SST variability in a slightly different MDR region (280ºE-310ºE, 5ºN-15ºN) and the Niño 3

region (210ºE-270ºE, 5ºS-5ºN) did not increase the skill score significantly, suggesting that this additional information may be redundant on account of it being already included in the vertical wind shear.

To assess optimality of predictors, sensitivity experiments are conducted for identifying the strongest zonal-wind shear and SST correlations of Atlantic hurricane counts over the Atlantic region. For sensitivity experiments, three wind shears are considered: the zonal wind difference at the level of 200 and 850 hPa, and 150 and 700 hPa ($(U_{200\ hPa}-U_{850\ hPa}$, $U_{150\ hPa}-U_{700\ hPa}$: only shown in Table-3.1), and the magnitude of the zonal wind difference at the level of 200 and 850 hPa ($|U_{200\ hPa}-U_{850\ hPa}|$). The influence of averaged wind shear in four regions is evaluated; here and in the SST box definitions, 'KW' refers to Kim and Webster (2010), 'KN' to Kim and Nigam, and 'VS' to Vecchi and Soden (2007b). The regions are marked in Fig. 3.1.

- KW-MDR_{Uz}: 260ºE-320ºE, 10ºN-20ºN (also defined earlier)
- KN-MDR_{Uz}: 270ºE-300ºE, 10ºN-20ºN
- VS-MDR_{Uz}: 300ºE-340ºE, 8ºN-15ºN
- VS-SER_{Uz}: 270ºE-320ºE,13ºN-25ºN

Likewise, the influence of SST variability in four regions of the Atlantic is assessed. The regions sample SST variability in both the tropical and extratropical basins, and are marked in Fig. 3.1

- KN-MDR_{SST}: 270ºE-313ºE, 7ºN-16ºN (tropical SST box)
- KW-MDR_{SST}: 280ºE-310ºE, 5ºN-15ºN (tropical SST box)
- KW-$NATL_{SST}$: 330ºE-350ºE, 35ºN-45ºN (also defined earlier; extratropical)
- KN-$NATL_{SST}$: 330ºE-350ºE, 38ºN-47ºN (extratropical box)

The influence of wind shear and SST on hurricane counts is examined in two periods: 1981-2009, for comparison with Kim and Webster's (2010) analysis, and 1958-2005, the target analysis period (the common period between NCEP reanalyses and IPCC-AR5 model simulations). To compare results as closely as possible with Kim and Webster's in the 1981-2009 period, the wind shear and SST indices are constructed exactly as in their analysis: wind shear from ERA40 from 1981 to 1988, and from ERA-interim from 1989 to 2009; SSTs from ERSSTv3 from 1981 to 2009.

Figure 3.1 depicts the spatial distribution of correlation coefficient between both wind shear and SST over the Atlantic and the observed hurricane numbers. The vertical wind shear ($U_{200hPa}-U_{850hPa}$), following our definition, has a wide and significant negative-correlation (overall, $R<-0.7$) with the hurricane numbers from the tropical East Pacific to the tropical Atlantic (Fig. 3.1a). While the shear of the magnitude of the zonal wind difference at the level of 200 and 850 hPa ($=|U_{200hPa}-U_{850hPa}|$), following Kim and Webster (2010)'s definition, has a relatively lower negative correlation (overall, $R<-0.6$) distributed mainly over the tropical Atlantic (Fig. 3.1b). For SST, the correlation structure (Figs. 3.1d-e, especially panel *d*) resembles the Atlantic Meridional Mode (AMM) which was shown to be significantly linked to the Atlantic hurricane activity (Kossin and Vimont 2007, Vimont and Kossin 2007); Saunders and Lea (2008) have also argued for a link between Atlantic warming and the increasing hurricane counts in that basin. The SST correlations also exhibit close resemblance with the Atlantic Multidecadal Oscillation's SST structure (Guan and Nigam 2009), consistent with the known link between AMO and Atlantic TC counts (e.g., Nigam and Guan 2011).

For the more extended 1958-2005 period, the magnitude of the wind shear and SST correlation coefficients is smaller, not surprisingly, as reflected also in some shrinkage of the shaded areas. Interestingly, the direct linkage of Atlantic hurricane counts with eastern tropical Pacific SSTs is greatly reduced in the extended period analysis. This is not necessarily an indication of reduced ENSO influence in the longer period but just a reflection of more energetic ENSO activity in recent decades. As noted earlier, ENSO's influence on Atlantic TC counts is likely exerted through modulation of wind shear over the MDR region of the tropical Atlantic. All correlation coefficients remain still statistically significant at 95% significance level ($p < 0.05$).

Table-3.1 shows the 200-850 hPa vertical wind shear ($U_{200\ hPa} - U_{850\ hPa}$) to have the best correlation coefficient values (−0.826 and −0.695, shown in blue) for both periods, while the 150-700 hPa zonal wind shear ($U_{150\ hPa} - U_{700\ hPa}$) has the lowest correlations of the three. The magnitude of the 200-850 hPa wind shear, $|U_{200\ hPa} - U_{850\ hPa}|$, is shown to have a marginally lower correlation than the highest one in all areas excepting the VS−MDR region. In the shorter period, the highest wind shear correlations are found in the KN−MDR_{Uz} region, and the highest SST ones in the KN-$NATL_{SST}$ region. These correlations are slightly higher than those for the corresponding regions in Kim and Webster (2010), and the wind-shear ones considerably higher than those noted in Vecchi and Soden (2007b). Also, and interestingly, SSTs in the midlatitude Atlantic basin are more strongly connected with Atlantic TC counts than those in the tropical Atlantic itself; at some odds with expectations rooted in dominance of the thermodynamic control of regional SSTs.

In the longer period (1958-2005) analysis, the 200-850 hPa wind shear is again most strongly correlated but in the Kim and Webster identified region in the tropical Atlantic; these authors, of course, considered not the shear, but its magnitude which is not as strongly correlated (cf. Table 3.1). In the longer period analysis, SSTs in the tropical Atlantic exert considerably more influence on TC counts than those in the midlatitude basin, consistent with canonical understanding.

Table-3.2 provides the results of the sensitivity of the Atlantic TC count reconstruction to various spatial averaging regions for the wind shear and SSTs in both the recent and extended analysis periods. The sensitivity is indicated using the correlation coefficient between the observed and reconstructed TC counts, and from the Root Mean Square Errorr (RMSE) between the two time series.

In the shorter recent period (1981-2009), the closest reconstruction is obtained from the MDR wind shear (KN-MDR_{Uz}) and midlatitude basin SSTs (KN-$NATL_{SST}$); the correlation coefficient is 0.86 and a RMSE of 1.5. In the longer period (1958-2005), the highest correlation (0.74) and smallest RMSE (1.77) are obtained with the MDR wind shear (albeit in a slightly different domain, KW-MDR_{Uz}) and MDR SSTs (KN-MDR_{SST}). It is interesting that almost all choices of averaging regions for wind shear and SSTs yield high correlations and low RMSE; for instance, in the extended period, correlations range from 0.732 to 0.741, while RMSE are in the 1.769-1.795 range.

3.3.2 Statistical modeling of Atlantic TC Counts

Based on the sensitivity experiments, two multi-linear regression models are built using best predictor-combinations of wind shear and SST in each period, which are KN-MDR_{Uz} and KN-$NATL_{SST}$, and KW-MDR_{Uz} and KN-MDR_{SST} in the shorter and

longer periods, respectively. The TC count variations generated by the statistical models are shown in Figure 3.2. The reconstruction by KN-MDR_{Uz} and KN-$NATL_{SST}$ (dashed red line), the best predictor-combination in the 1981-2009 period, well captures the observed hurricane numbers except in the years of 2001, 2005, and 2006. The same predictors (solid red line) are however not as effective in the extended period, as evident from the misfit in the earlier period (1958-1980). The optimal predictors in the extended period – KW-MDR_{Uz} and KN-MDR_{SST} – the best combination of predictors in the period 1958-2005 lead to closer reconstruction, as evident from the higher correlation (0.741 vs. 0.717) and lower RMSE (1.769 vs. 1.839), noted in the Fig. 3.2 legend.

The statistical models constructed for Atlantic TC counts are tested in an independent past-period (1949-1957). This period is among the earliest for which upper-air data was collected, predating the International Geophysical Year (1958) when coordinated upper-air observations became more common and routine. This independent sub-period is thus one with potentially more data uncertainties than any other in the analyzed record, especially in context of the 200-850 hPa wind shear. Notwithstanding this drawback, the TC counts reconstructed in this independent sub-period are compared with the observed counts in Fig. 3.3. The zonal wind shear used in the reconstruction comes from NOAA's NCEP reanalyses since the ERA40 data commences in 1958. The hindcast/reconstruction by the regression model using KN-MDR_{Uz} and KN-$NATL_{SST}$ has a higher correlation of 0.769 (and also a higher RMSE of 3.006) with the observed counts than the one based on KW-MDR_{Uz} and KN-MDR_{SST}. Both models will be used to reconstruct TC counts from the IPCC-AR5 simulations of the 20th century climate, as one

model leads to higher correlations while the other to lower RMSE in the independent sub-period.

3.4 Reconstruction of Atlantic hurricane counts from IPCC-AR5 simulations of 20th century SST and wind shear

The predictors identified from analyses of observations for the second half of the 20th century are used in this section to reconstruct hurricane counts from *simulated* values of SST and wind shear; the averaging domain for these variables remain the same as before, i.e., remains based on prior observational analysis. Using the same two sets of predictors (and predictor definitions), different multivariate regression models are constructed for the IPCC-AR5 climate system models: One regression model for each IPCC-AR5 model, totaling ten regression models (2 statistical models x 5 IPCC-AR5 simulations).

In the IPCC archives, there exist several 20th century simulations from each AR5 climate system model, i.e., an ensemble of simulations, with the number of ensemble members range from 3 in case of the MPIESMLR and 10 for the HADCM3 model. The availability of several ensemble simulations from each model provides interesting investigative opportunities: For example,

- Analysis of the *ensemble-mean* simulation allows one to focus on the long-term trend since averaging across ensemble members leads to suppression of interannual-to-multidecadal variability as each ensemble member – a coupled ocean-atmosphere-land-surface-cryosphere simulation – is potentially in a

different phase of natural variability. The ensemble-mean simulations are used in developing the statistical models for Atlantic TC counts in this chapter (Chapter 3), in view of our interest in investigating the long-term trend in hurricane counts. These statistical models will this be unable to represent count variations on interannual-to-multidecadal timescale, of course, by design.

- On the other hand, use of *all* the ensemble members in statistical reconstruction of TC counts should allow for a modeled temporal structure rich in interannual-to-multidecadal variability. This approach is adopted in Chapter 4 where decadal forecast of TC counts is of primary interest.

In the following, the *ensemble-mean* simulation of 20th century climate – specifically, 200-850 hPa wind shear and SSTs during the 1958-2005 period – produced by each IPCC-AR5 model is used to develop a statistical model for TC counts. As climate simulations from five IPCC-AR5 models are analyzed, 5 statistical models are developed for each predictor set. Figure 3.4 shows the performance of the statistical models for both predictor sets, by first showing the unweighted, multi-model average of the reconstructed counts in the 1958-2005 period. The reconstructed counts are devoid of interannual-to-multidecadal variations, not unexpectedly; they however do reflect, reasonably, the observed long-term trend in counts. Both predictor sets (thick red and blue lines) yield qualitatively similar results but with the optimal predictors for the latter period (thick red line) yielding a slightly weaker increasing linear trend in counts, as indicated in the figure legend. The linear trend in modeled TC counts is further investigated in Figure 3.7.

Specifically, the KN-MDR$_{Uz}$ and KN-NATL$_{SST}$ based count reconstruction is correlated at 0.460 with observations (with RMSE of 2.446) while the model based on KW-MDR$_{Uz}$ and KN-MDR$_{SST}$ is correlated at 0.392 (with RMSE of 2.440), in accord with the earlier analysis. These correlations are notably less than those of the statistical models based on the single record of wind shear and SST observations (~0.7), which allows the latter models to represent both the long-term trend as well as interannual-to-multidecadal variability in counts.

It is of some interest to examine the basis of TC count reconstruction using the IPCC-AR5 *ensemble-mean* climate simulations. Figure 3.5a-e shows low correlations ($|R| < 0.3$) for the wind shear predictor; even positive correlation in one case (MRI-CGCM3). Again, this likely reflects, not weakness of the models, but the important role of interannual-to-multidecadal variability in generating correlations between TC counts and Atlantic wind shear, such as those manifest in Fig. 3.1a-c. The SST correlations in the ensemble-mean simulations are shown in Fig. 3.5f-j, and are notable for the absence of strong correlations in the western tropical Atlantic basin, especially the Caribbean Seas (as in observations, cf. Fig. 3.1d-e).

The statistical models developed from ensemble-mean simulations of wind shear and SST are compactly shown using the scatter-plot in Figure 3.6; the 5 red and 5 blue dots depict the regression coefficients of the two optimal predictors in the recent and extended period, respectively; concentric circles denote the mean regression coefficients (the average of 5 dots). The regression coefficients of the observationally-rooted models are indicated by solid red and blue squares. All regression models – observation as well as the IPCC simulation based – exhibit +ve coefficients for the SST predictors (KN-

NATL and KN-MDR), indicating that warmer SSTs in these regions lead to increased Atlantic TC counts. The sensitivity to SSTs ranges from being near-zero in the MPIESMLR model to phenomenal in the MRICGCM3; the sensitivity to local (i.e., MDR) SSTs is, understandably, larger.

In contrast with the accord on the sign of the SST regression coefficient, the wind shear coefficient exhibits considerable scatter across both the $y>0$ and $y<0$ right quadrants. This scatter leads to the weakly positive regression coefficients on average, in both analysis periods – in contrast with the significantly negative wind shear regression coefficients in observation-based models. This sign-disparity could result from the suppression of interannual-to-multidecadal variability during construction of statistical models based on IPCC simulations; this would have to be ruled out before the disparity is attributed to the coupled model simulation deficiencies.

In summary, the regression models for Atlantic TC counts based on the IPCC-AR5 simulations show a statistically significant correlation (0.460 and 0.392: both p-value<0.05) with the observed counts, especially the model constructed with the KN-MDR_{Uz} and KN-$NATL_{SST}$ predictors. This model (red dots and concentric circle) is physically closer to the observation based statistical model in the U_z –SST phase space (cf. Fig. 3.6).

The linear trend in the TC counts reconstructed from the IPCC-AR5 simulations is shown in Fig. 3.7; the KN-MDR_{Uz} and KN-$NATL_{SST}$ predictor set is used for this analysis. For each AR5 model, the statistical TC count model is based on the *ensemble-mean* simulation of wind shear and SST, as noted earlier. To provide an estimate of uncertainty, the 'fixed' statistical model is used to construct TC counts from all ensemble

members of this AR5 model's 20th century simulation. The spread between the maximum and minimum hurricane counts predicted by the statistical model is shaded in yellow, with the yellow ribbon visually denoting the uncertainty in TC counts. The red line denotes the ensemble-mean counts, and the dashed red line the linear trend in TC counts.

Three of the five TC count models based on the IPCC-AR5 simulations generate statistically significant, positive, and 'realistic' linear trends in the 1958-2005 period (cf. Table 3.3); the model based counts are plotted in the left column of Figure 3.7:

- CCSM4 (with 6 ensemble members): 5.04±1.27 counts/century
- GFDLCM3 (with 5 ensemble members): 3.72±1.48 counts/century
- HADCM3 (with10 ensemble members): 3.79±1.42 counts/century

These trends should be compared with observational estimates:

- Trend in observed TC count data: +4.88±5.32 counts/century
- Trend in observation-based statistical model: 4.01±3.77 counts/century

All three models showing statistically significant trends in TC counts indicate increasing trend in the 1958-2005 period, with similar count-spread. The remaining two statistical models generate weakly positive trends but do not pass the statistical significance test.

Further inspection of Table-3.3 reveals that in almost all cases, including the reanalysis record, the linear trend in wind shear (KN-MDR_{Uz}) cannot be estimated with confidence. The trend in extratropical Atlantic SST (KN-$NATL_{SST}$), on the other hand, is almost always estimable at the 95% significance level, and it is this predictor that allows

for the estimation of the statistically significant linear trend in TC counts in most cases; the SST predictor exerts greater influence (cf. Fig 3.6).

3.5 Projection of Atlantic hurricane counts based on IPCC-AR5 model projections of wind shear and SSTs

Several recent modeling studies (and related analysis) project a reduction in TC activity in the 21st century, based largely on the significantly increased wind-shear over MDR in the IPCC-AR4 projections (Garner et al., 2009; Vecchi and Soden, 2007b; Gualdi et al., 2008; Bengtsson et al., 2007; Zhao et al., 2009). As noted earlier, many of these studies analyze only the IPCC 21st century projections, and not 20th century simulations that can provide a reading on model performance. Our Table-3.3 shows the 20th and 21st century trends of vertical wind-shear (KN-MDR$_{Uz}$), SST (KN-NATL$_{SST}$), and the reconstructed and projected hurricane counts from all 5 model simulations and projections using all publicly available ensemble members.The statistical significance of the trend in hurricane counts was evaluated using the student's t-test and the 95% significance level; the trends that passed the t-test are depicted in bold face: red for positive, blue for negative trends, and the rest in black.

The analysis now seeks to address the seminal question in hurricane modeling under global warming: Will TC counts in the Atlantic basin increase with increasing greenhouse gas concentrations, and related warming of the planet? The statistical models for TC counts were, in fact, constructed to directly address this question, by using the *ensemble-mean* simulations of wind shear and SSTs as predictors. Moreover, by

examining the performance of these models in the 1958-2005 period, this study will allow us to consider some projections with more confidence than others.

For the IPCC-AR5 21st century (2006-2100) projections, in the third row of Table-3.3), the wind-shear trend is statistically significant in only two cases (CCSM4 and MPIESMLR), and positive in both of those. The wind shear is *negative* in 2 of the 5 projections, but insignificant: −1.70 ±1.71 (GFDL-CM3.0) and −0.07 ±4.77 (HadCM3.0). HadCM3 – the only model exhibiting statistically-significant and correct-signed wind shear in the 20th century – does not show a significant wind shear trend in the 21st century projections. In contrast, the SST trend in all five climate projections is positive and statistically significant, with the average trend being +1.99 ±0.16 ºC/century.

The 21st century trend in TC counts inferred from the IPCC projections of wind shear and SST are shown in Table-3.3 (third row). Four of the five projected count-trends are statistically significant, and all positive. If the 21st century projections of the trend in TC counts are sub-selected based on the 20th century model performance (Table-3.3 second row; model-observation intercomparison), only three projections survive: CCSM4.0, GFDL-CM3.0, and HadCM3.0. The mean 21st century TC-count trend from this subset is +4.77 ±0.50 counts /century, and results largely from the SST warming trend. For these 3 models, the wind-shear trend is significant in only one (CCSM4.0), and positive. The increasing trend in counts must therefore result from the dominance of the SST effect. The sub-selection of statistically significant results based on the corresponding models performance in producing realistic and correctly signed count-trends in the 1958-2005 period, increasing confidence in the projected count trends.

From these results, one can conclude that there is no unequivocal evidence from the five analyzed IPCC model projections for the 21st century for increasing wind-shear over MDR! In contrast, there is sufficient evidence for increasing TC counts based on the increasing trend in Atlantic SSTs in the IPCC-AR5 21st century projections under RCP4.5 scenario. This analysis argues against equal weighting of all model projections.

3.6 Summary and Concluding Remarks

Atlantic Tropical Cyclone (TC) counts are reconstructed in the 20th century and projected in the 21st century from statistical modeling with SST and vertical shear of the zonal wind in the Atlantic basin as predictors. The predictors are obtained from both observations and IPCC-AR5 simulations of 20th century climate, and from the IPCC-AR5 projections of 21st century climate. The need for statistical modeling of tropical cyclone counts (or the costlier and more challenging dynamical downscaling) is patent as the IPCC-class climate system models cannot realistically model regional hydroclimate, let alone tropical cyclones, in part, due to the coarse horizontal resolution of the component atmospheric models.

The principal findings in this chapter are

- Modified definition of zonal wind shear – actual value rather absolute value of U200-U850 and a slightly different geographical averaging area – results in it becoming a more effective predictor of Atlantic hurricane counts. Focusing on the actual rather than absolute value of the shear (as in Kim and Webster 2010) is key to this improvement.

- Modified predictor definitions/averaging domains led to remarkable reconstruction of Atlantic hurricane counts in both the training and independent periods; more closely than ever before, as revealed from comparison with Kim and Webster's (2010) analysis.
- Statistical models for hurricane counts constructed using predictors from the IPCC-AR5 ensemble-mean simulations of 20th century climate exhibit similar sensitivity to Atlantic SSTs but, often, weaker and opposite-signed sensitivity to the tropical Atlantic wind-shear as the observations based statistical models.
- Modeling of Atlantic hurricane activity with IPCC-AR5 predictors shows a stronger count-trend in the 21st century (RPC4.5 scenarios) than in 20th century, principally, from the increasing SSTs.
- The AR5 models disagree on the sign and magnitude of the 21st century trend in zonal-wind shear. As such, there is no unequivocal evidence for an increasing zonal wind shear in the 21st century projections, and thus limited potential for off-setting the count-increase from SST effects.

3.7 Tables

Table-3.1: Correlation coefficients between the time series of zonal wind shear and SST of reanalyses and the Atlantic Hurricanes observation; the area averaged wind shear and SST are averaged from July to October (JASO) for the periods 1981-2009 (the second row) and 1958-2005 (the third row). Colored numbers depict the name of averaged area and the highest correlation coefficient among the designated areas for sensitivity experiment in two periods; blue is for zonal wind shear and red is for SST.

Period	Variable	Area			
1981-2009		KN-MDR$_{Uz}$	KW-MDR$_{Uz}$	VS-MDR	VS-SER
	$U_{200\ hPa}$-$U_{850\ hPa}$	**-0.826**	-0.808	-0.658	-0.741
	$\lvert U_{200\ hPa}-U_{850\ hPa} \rvert$	-0.821	-0.807	-0.721	-0.737
	$U_{150\ hPa}$-$U_{700\ hPa}$	-0.787	-0.764	-0.595	-0.718
	SST	KN-MDR$_{SST}$	KW-MDR$_{SST}$	KN-NATL$_{SST}$	KW-NATL$_{SST}$
		0.639	0.624	**0.681**	0.667
1958-2005		KN-MDR$_{Uz}$	KW-MDR$_{Uz}$	VS-MDR	VS-SER
	$U_{200\ hPa}$-$U_{850\ hPa}$	-0.687	**-0.695**	-0.521	-0.628
	$\lvert U_{200\ hPa}-U_{850\ hPa} \rvert$	-0.657	-0.670	-0.560	-0.629
	$U_{150\ hPa}$-$U_{700\ hPa}$	-0.661	-0.667	-0.434	-0.613
	SST	KN-MDR$_{SST}$	KW-MDR$_{SST}$	KN-NATL$_{SST}$	KW-NATL$_{SST}$
		0.686	0.675	0.526	0.500

Table-3.2: Correlation coefficients and RMSE between the time series of the observed Atlantic hurricanes and the reconstruction by reanalyses; the wind shear and SST are averaged from July to October (JASO) over the periods 1981-2009 and 1958-2005.

1981-2009	Predictors	KN-MDR_{Uz} + KN-NATLsst	KN-MDR_{Uz} + KW-$NATL_{SST}$	KW-MDR_{Uz} + KN-$NATL_{SST}$	KW-MDR_{Uz} + KW-$NATL_{SST}$
	CORR(RMSE)	0.861 (1.496)	0.852 (1.541)	0.853 (1.538)	0.836 (1.615)
1958-2005	Predictors	KN-MDR_{Uz} + KN-MDRsst	KN-MDR_{Uz} + KW-MDR_{SST}	KW-MDR_{Uz} + KN-MDR_{SST}	KW-MDR_{Uz} + KW-MDR_{SST}
	CORR(RMSE)	0.737 (1.781)	0.732 (1.795)	0.741 (1.769)	0.737 (1.781)

* KN-MDR_{Uz} + KN-$NATL_{SST}$ in 1958-2005 : 0.717 (1.839)

Table-3.3: The linear trend in vertical shear of the seasonal zonal wind over KN-MDR Region of the tropical cyclones in the Atlantic basin, SST over KN-NATL in the North Atlantic basin, and reconstructed hurricanes in the period of 1958-2005. The *seasonal (JASO)* linear trend in the shear SST, and reconstructed hurricanes, noted in units of m/s/century, ºC/century, and number/century, respectively; the 95% confidence interval (CI) is noted in parenthesis. The first row documents the **observed** shear trend in recent periods (1958-2005) from reanalysis (ECMWF ERA40 and ERA-INTERIM for zonal wind shear and NOAA ERSSTv3 for SST). The second row documents the linear shear-trend in the **historical climate simulations** (1958-2005) from five IPCC-AR5 models (NCAR-CCSM4.0, GFDL-CM3.0, HadCM3.0, MPI-ESMLR, and MRI-CGCM3.0), with varying number of ensemble members (also noted), while the third row does the same for the **rcp4.5 climate projections** (2006-2100) obtained from the same models. Trends deemed statistically significant (i.e., when it passes student's t-test at 95% of significance level) are bold-faced; positive (negative) trends are in red (blue).

Atmospheric Reanalyses (1958-2005)	$KN\text{-}MDR_{Uz}$	-3.31(±5.62)					
	$KN\text{-}NATL_{SST}$	**1.47**(±0.75)					
	RECON.	**4.01**(±3.77)					
		CCSM4	GFDLCM3	HADCM3	MPIESMLR	MRICGCM3	Ensemble Mean
IPCC AR5 Models (1958-2005)	# of Ensemble members	6	5	10	3	5	
	$KN\text{-}MDR_{Uz}$	1.77(±1.93)	-0.70(±2.72)	**2.84**(±2.39)	3.63(±5.15)	-0.95(±1.87)	1.32(±1.40)
	$KN\text{-}NATL_{SST}$	**1.56**(±0.42)	**1.56**(±0.60)	**0.94**(±0.43)	**0.82**(±0.64)	**0.71**(±0.56)	**1.12**(±0.27)
	RECON.	**5.04**(±1.27)	**3.72**(±1.48)	**3.79(**±1.42)	0.01(±0.18)	0.81(±1.70)	**2.67**(±0.71)
IPCC AR5 Models (2006-2100)	# of Ensemble members	6	1	10	3	1	
	$KN\text{-}MDR_{Uz}$	**1.53**(±0.76)	-1.70(±1.71)	-0.07(±4.77)	**3.81**(±1.90)	0.96(±1.60)	**-0.98**(±0.74)
	$KN\text{-}NATL_{SST}$	**0.84**(±0.16)	**2.94**(±0.37)	**1.43**(±0.73)	**0.91**(±0.27)	**1.77**(±0.41)	**1.99**(±0.16)
	FCST.	**2.85**(±0.49)	**7.08**(±0.99)	**5.11**(±2.73)	0.02(±0.08)	**4.19**(±1.20)	**3.21**(±0.39)

3.8 Figures

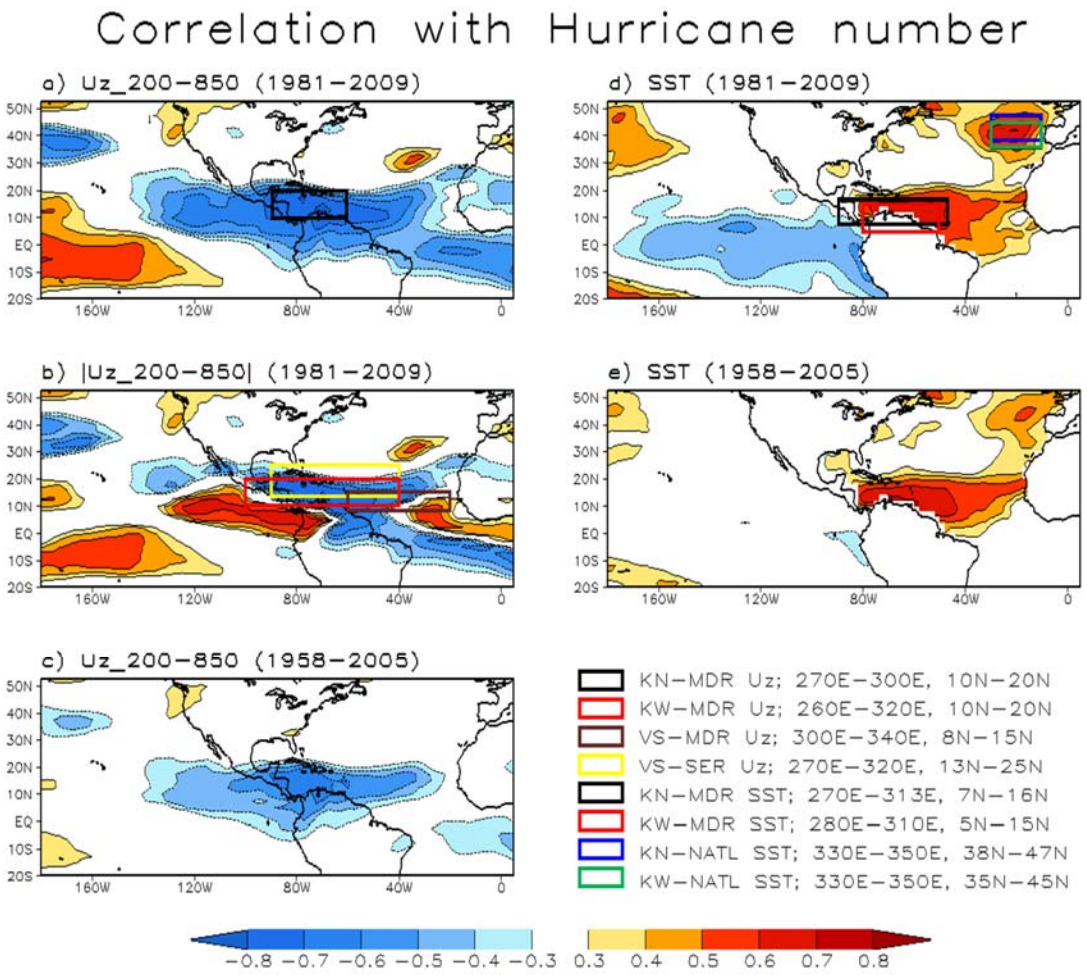

Figure 3.1: The spatial distribution of correlation coefficients between the observed number of Atlantic hurricane and (left) zonal-wind shear and (right) SST of reanalyses: (a) $Uz_{200\text{-}850}$ ($U_{200\ hPa}$-$U_{850\ hPa}$), (b) $|Uz_{200\text{-}850}|$ ($|U_{200\ hPa}$-$U_{850\ hPa}|$) are over the period 1981-2009, (c) $Uz_{200\text{-}850}$ ($U_{200\ hPa}$-$U_{850\ hPa}$) over the period 1958-2005, (d) SST over the period 1981-2009, (e) SST over the period 1958-2005. All correlation coefficients are averaged from July to October over each period, and pass the significance test at 95% significance level ($p<0.05$).

* The areas are; Kim and Webster (2010) defined MDR for zonal-wind shear, MDR for SST, and the North Atlantic for SST as the area of 260ºE-320ºE and 10ºN-20ºN (hereafter, $KW\text{-}MDR_{Uz}$, red box in b), 280ºE-310ºE, 5ºN-15ºN (hereafter, $KW\text{-}MDR_{SST}$, red box in d), 330ºE-350ºE, 35ºN-45ºN (hereafter, $KW\text{-}NATL_{SST}$, green box in d), respectively. Vecchi and Sodden, 2007b defined MDR and SER for zonal-wind shear as the area of 300ºE-340ºE, 8ºN-15ºN (hereafter, $VS\text{-}MDR_{Uz}$, brown box in b) and 270ºE-320ºE, 13ºN-25ºN (hereafter, VS-SERUz, yellow box in b). Kim and Nigam define MDR for zonal-wind shear, MDR for SST, and the North Atlantic for SST as the area of 270ºE-300ºE, 10ºN-20ºN (hereafter, $KN\text{-}MDR_{Uz}$, black box in a), 270ºE-313ºE, 7ºN-16ºN (hereafter, $KN\text{-}MDR_{SST}$, black box in d), and 330ºE-350ºE, 38ºN-47ºN (hereafter, $KN\text{-}NATL_{SST}$, blue box in d), respectively.

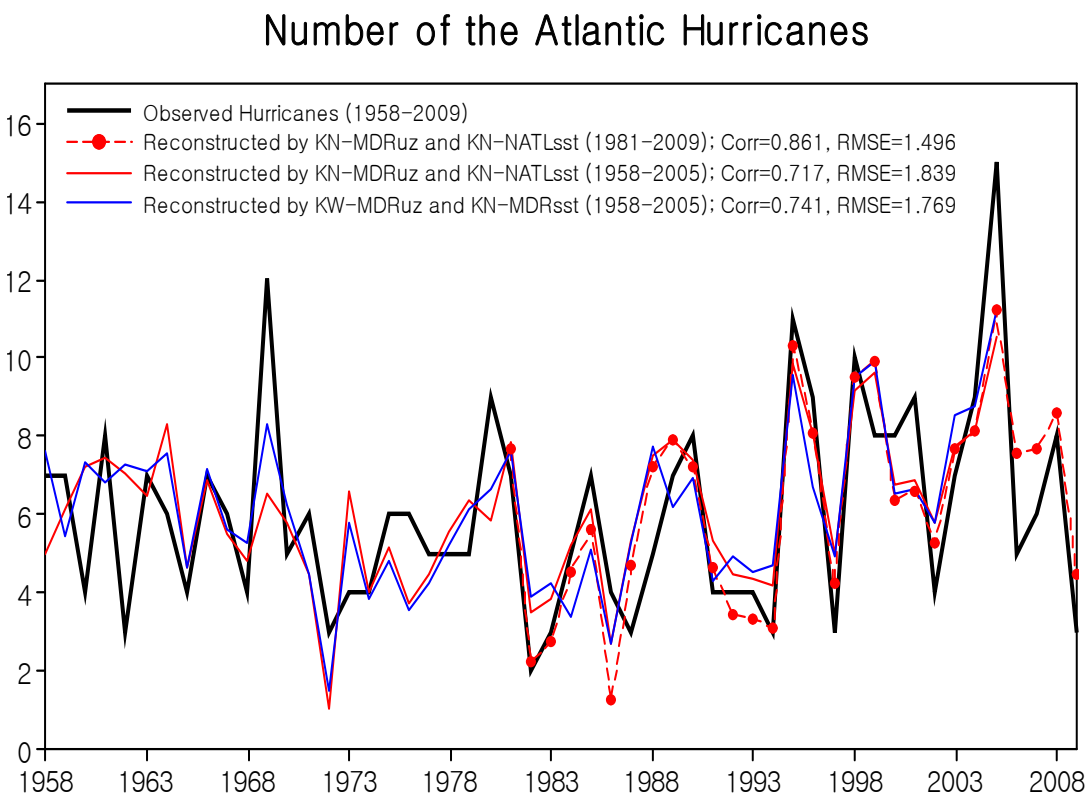

Figure 3.2: The time series of the observed Atlantic hurricanes (black), the reconstructed hurricanes by KN-MDR_{Uz} and KN-$NATL_{SST}$ of reanalyses over the period 1981-2009 (red dash-dotted), by KN-MDR_{Uz} and KN-$NATL_{SST}$ over the period 1958-2005 (red solid), and by KW-MDR_{Uz} and KN-MDR_{SST} over the period 1958-2005 (blue solid); the correlation coefficients and RMSE value are noted in the legend.

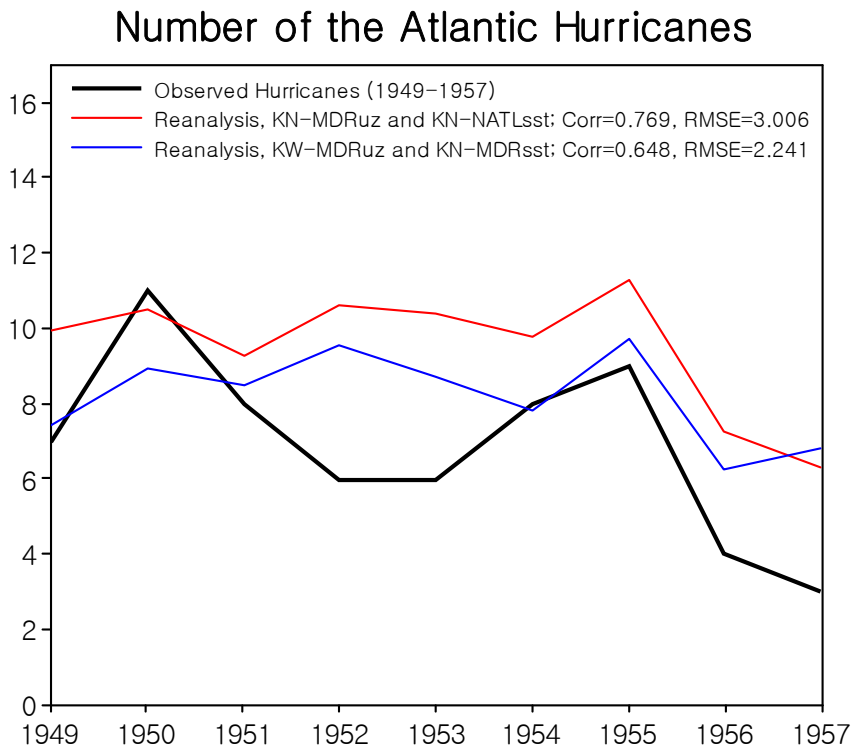

Figure 3.3: The time series of the observed Atlantic hurricanes (black) and the reconstructed hurricanes from reanalyses of NOAA's NCEP for zonal wind shear and NOAA's ERSST V3 for SST over the period 1949-1957: the reconstruction of KN-MDR_{Uz} and the KN-$NATL_{SST}$ is shown in red and of KW-MDR_{Uz} and KN-MDR_{SST} is shown in blue; the correlation coefficients and RMSE value are noted in the legend.

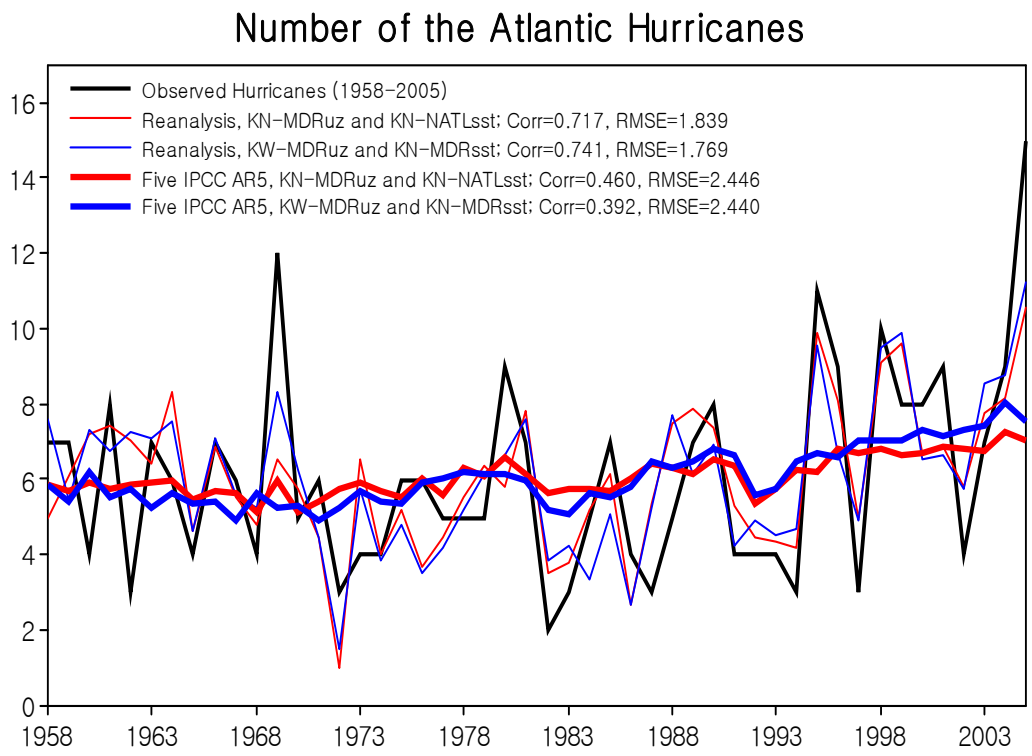

Figure 3.4: The time series of the observed Atlantic hurricanes (black), reconstructed hurricanes from reanalyses, which is by KN-MDR_{Uz} and KN-$NATL_{SST}$ (red dashed) and by KW-MDR_{Uz} and KN-MDR_{SST} (blue dashed), and ensemble mean of reconstructed hurricanes from five IPCC-AR5 models (NCAR-CCSM4.0, GFDL-CM3.0, HadCM3.0, MPI-ESMLR, and MRI-CGCM3.0); the wind shear and SST are averaged over the area KN-MDR_{Uz} and KN-$NATL_{SST}$ (red solid) and KW-MDR_{Uz} and KN-MDR_{SST} (blue solid) over the period 1958-2005, respectively. The correlation coefficients and RMSE value are noted in the legend.

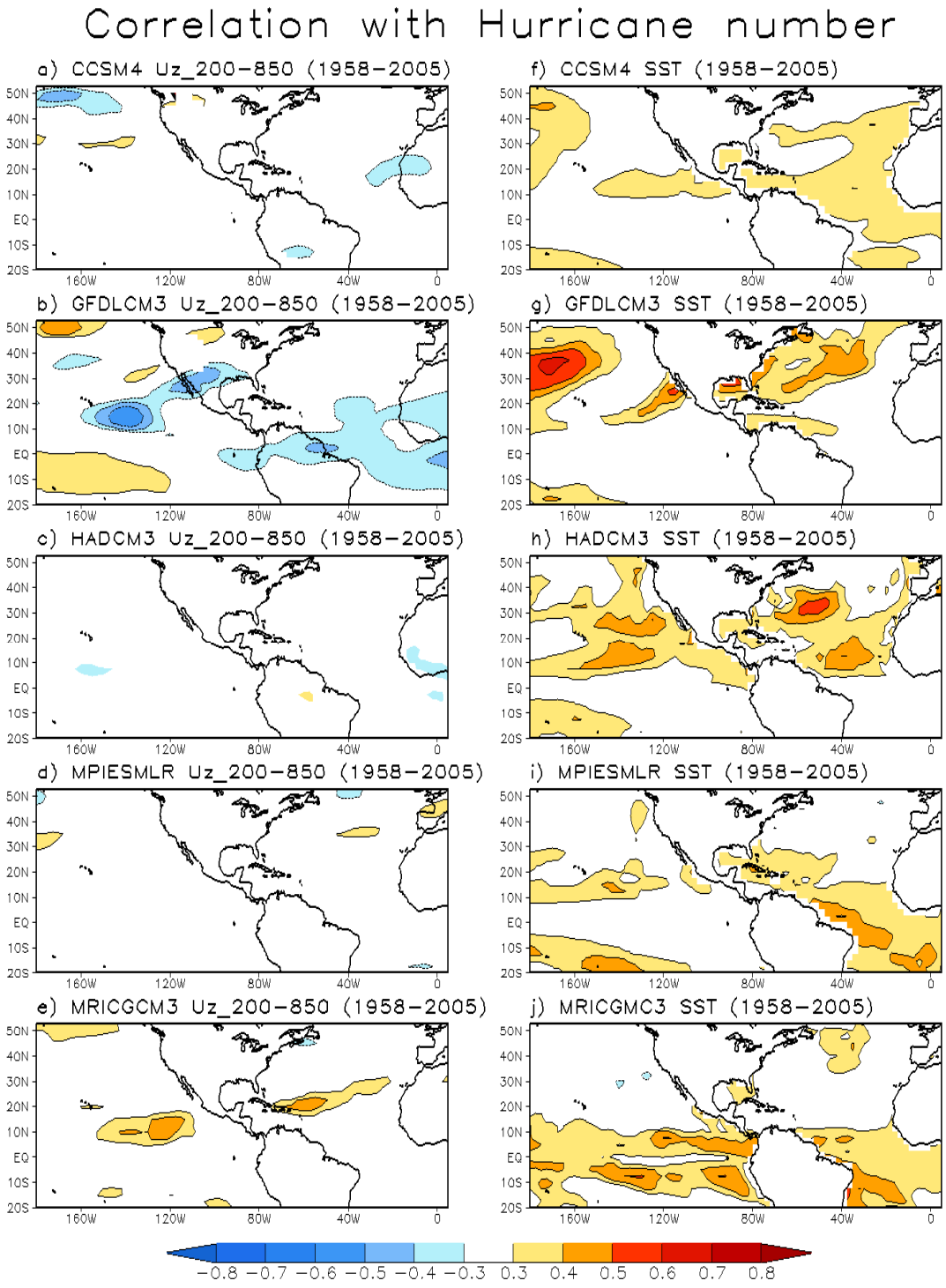

Figure 3.5: The spatial distribution of correlation coefficients between the observed number of Atlantic hurricane and zonal-wind shear, $Uz_{200\text{-}850}$ ($U_{200\ hPa}$-$U_{850\ hPa}$), and SST of five IPCC-AR5 models (a, f) NCAR-CCSM4.0, (b, g) GFDL-CM3.0, (c, h) HadCM3.0, (d, i) MPI-ESMLR, and (e, j) MRI-CGCM3.0. All correlation coefficients are averaged from July to October over the period 1958-2005.

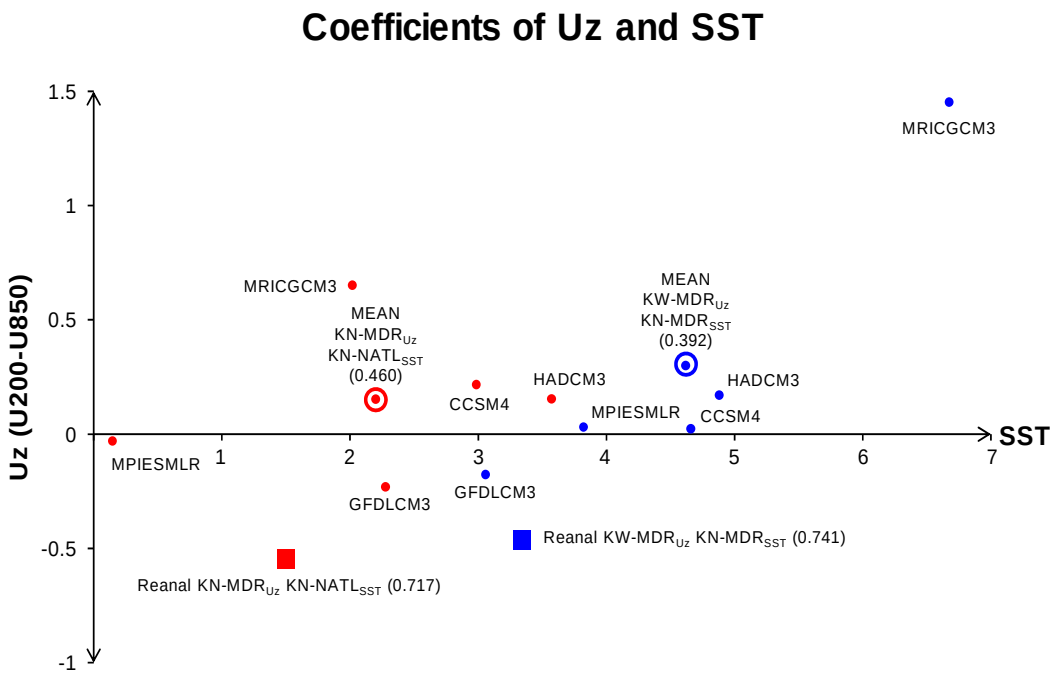

Figure 3.6: The scatter plot of Uz and SST coefficients of multi-regression model from reanalyses with KN-MDR$_{Uz}$—KN-NATL$_{SST}$ (red rectangle) and KW-MDR$_{Uz}$—KN-MDR$_{SST}$ (blue rectangle) and from five IPCC-AR5 models with KN-MDR$_{Uz}$—KN-NATL$_{SST}$ (red dot) and KW-MDR$_{Uz}$—KN-MDR$_{SST}$ (blue dot) for the period 1958-2005, respectively. The mean regression coefficients of IPCC-AR5 models are shown in circle.

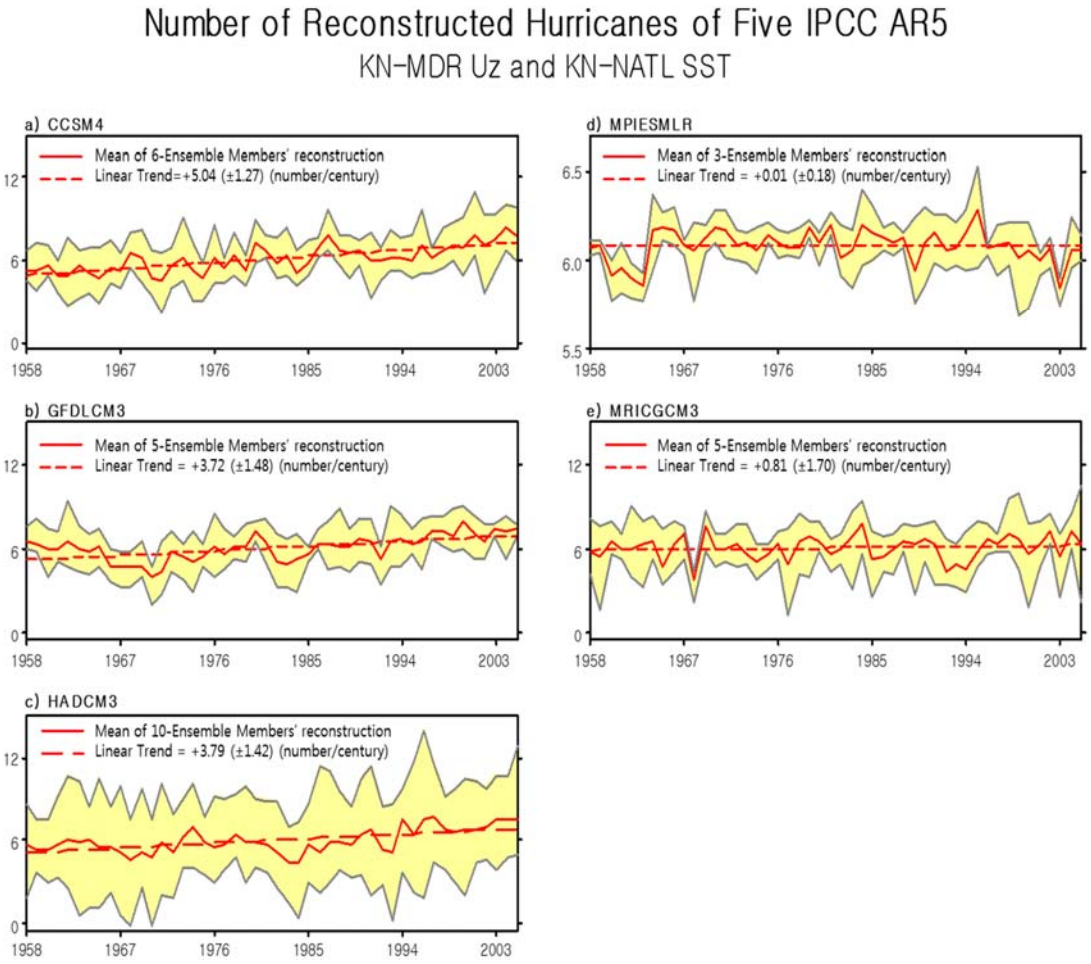

Figure 3.7: The time series the Atlantic hurricanes reconstructed by KN-MDRUz and KN-NATLSST of five IPCC-AR5 models and the linear trends over the period 1958-2005. The ensemble mean of reconstructed hurricane numbers is shown in red-solid line and the corresponding linear trend and confidence interval are shown in red-dashed line in (a) CCSM4.0, (b) GFDL-CM3.0, (c) HadCM3.0, (d) MPI-ESMLR, and (e) MRI-CGCM3.0; the number of ensemble members and trend value are noted in the legend. The maximum and minimum of each model's reconstructed hurricanes are shaded in yellow and enveloped grey-solid line.

Chapter 4: Improved Statistical Modeling of the Atlantic Hurricane Activity based on the IPCC-AR5 20th Century Simulations and 21st Century Projections

4.1 Introduction

TC activity depends on three representative dynamic and thermodynamic factors: (1) vertical wind shear, (2) thermal energy related to SST, and (3) moist static instability (Gray 1968, 1975). TCs intensify as air at low altitudes is drawn toward the low pressure at the center of the TC while absorbing heat and moisture from the ocean. This heat is subsequently released as the air rises in the eyewall (Gray 1975; Emanuel 1986). The resulting decrease of inner core pressure leads to further convergence and heat release. This process depends both on structural properties of the TC and on environmental properties of the above mentioned dynamic and thermodynamic factors.

The vertical wind shear induced asymmetry of hurricane structure is deadly for TC growth because it renders the concentration of heat through the entire troposphere quite difficult (Gray 1968). A significant amount of vertical tilt due to large wind shear makes a coupling of the upper- and lower-level cyclone, not the coupling of lower-level cyclone and the upper-level anticyclone (Wang and Holland 1996). Also, mid-level warming associated with the vortex tilt (making the coupling of the upper- and lower-level cyclone) will not only lead to a decrease in convection near the low-level center, but it will also lead to increased convection outside the eyewall, which would further disrupt

storm symmetry and circulation (Jones 1994, DeMaria 1996). Furthermore, a large ventilation of heat away from the developing disturbance and the condensational heat released by the cumulus convection to the upper troposphere was quickly advected in a different direction relative to the heat released at lower levels (Gray 1968). The loss of heat in the core would lead to a weaker TC by increasing the inner core pressure (Frank and Ritchie 2001, Knaff et al. 2004).

The hurricane intensity in the Atlantic is closely related to SST variations in the MDR, where ocean waters above 26.5 ºC are generally required for TC formation (Gray 1979). The North Atlantic SST plays an important role on driving TC intensity (Landsea et al., 1999; Knight et al., 2006; Zhang and Delworth, 2006; Trenberth and Shea, 2006). Saunders and Lea (2008) showed that a 0.5 ºC increase in SST is associated with a 40% increase in hurricane intensity and frequency. TC intensity changes to SST increases could be underestimated by an increase in category 4 and 5 TCs by about 80%, as indicated by the ensemble projection of CMIP3 models (Bender et al. 2010)

The effect of atmospheric static stability on hurricane activity has been considered somewhat minor compared to some other factors. Change of tropical atmospheric stability may, however, be relatively large in some climate scenarios (Shen et al. 2000). Static stability is the atmospheric, thermodynamic indicator of a fluid becoming unstable or stable due to the effects of buoyancy neglecting all other inertial effects of motion. The troposphere must be potentially unstable to sustain convection for an extended period. High static stability is an adverse influence on TC intensity (DeMaria et al. 2001; Shen et al. 2000), as it both suppresses deep convection during cyclogenesis and reduces the potential intensity (Emanuel 1986, Holland 1997). Shen et al. (2000)

stated that hurricane intensity is more sensitive to lapse rate and SST changes over a warmer region with a more unstable lapse rate than over a colder region with a less unstable lapse rate.

This chapter focuses on the effect of static stability as well as zonal-wind shear and SST on Atlantic hurricane activity, especially on major hurricanes, development of advanced multi-variate regression models with a higher prediction performance than previously developed statistical hurricane prediction models, and the predictability for Atlantic hurricane activity with the five leading IPCC-AR5 models. Data sets are briefly discussed in section 4.2, development of statistical model in section 4.3, reconstruction of Atlantic hurricanes based on reanalyses and IPCC-AR5 model simulations in section 4.4, and the prediction of Atlantic hurricane activity by IPCC-AR5 model projections in section 4.5.

4.2 Data sets

Monthly-mean zonal winds at the 200 hPa and 850 hPa vertical levels and atmospheric temperature for calculating potential temperature and static stability were obtained from the European Centre for Medium-Range Weather Forecasts (ECMWF) Re-Analysis dataset (ERA-40; Uppala et al. 2005) for a 41-year (1958-1988) period, and ERA interim (Berrisford et al., 2009) for a 21-year (1989-2010) period. Monthly-mean Sea Surface Temperature (SST) was from the Extended Reconstructed Sea Surface Temperature Version 3 (ERSSTv3; Smith et al., 2008) for a 61-year (1958-2010) period. The hurricane data for Saffir-Simpson category storms 1 to 5 for a 61-year (1949-2009) period were downloaded from the NOAA Hurricane Best Track Database. The bimonthly

Multivariate ENSO Index (MEI) data for a 48-year (1958-2005) period was downloaded from the NOAA MEI database. MEI is the measure of monitoring ENSO based on the six main observed variables over the tropical Pacific. These six variables are: sea-level pressure, zonal and meridional components of the surface wind, sea surface temperature, surface air temperature, and total cloudiness fraction of the sky (Wolter 1987; Wolter and Timlin 1993).

The shear, SST, static stability and the Atlantic hurricane counts were analyzed in five IPCC-AR5 20th century simulations with historical runs – a 20th century experiment with all forcings and a 21st century projections with a medium mitigation scenario of Representative Concentration Pathway 4.5 (RCP4.5) – carbon dioxide concentrations stabilize at 650 ppmv near the year 2100 (approximately a CO_2 doubling at the end of the 21st century). Unlike the projection initialized from the end of freely evolving simulations of the historical period 1850-2005 and forced with specified CO_2 concentrations by RCP4.5 scenario, decadal prediction is initialized with observed ocean state in 2005 (decadal 2005) and no longer prescribed with CO_2 concentrations for the 10-year (2006-2015) integration, but forced with RCP4.5's CO_2 for the period 2016-2035. The gridded monthly-averaged data of RCP4.5 and decadal2005 was downloaded from the Program for Climate Model Diagnosis and Intercomparison. The analyzed models are from the US National Center for Atmospheric Research (NCAR-CCSM4.0), NOAA's Geophysical Fluid Dynamics Laboratory (GFDL-CM3.0), U.K. Meteorological Office's Hadley Center (HadCM3.0), Germany's Max Planck Institute (MPI-ESMLR), and Japan's Meteorological Research Institute (MRI-CGCM3.0).

The vertical wind shear is defined as the difference of the monthly 200 and 850 hPa winds ($=U_{200\ hPa}-U_{850\ hPa}$) following the commonly used levels (Goldenberg et al., 2001; Zhang and Delworth 2006; Vecchi and Soden 2007b). The static stability parameter (Sp) is defined as the negative sign of atmospheric temperature multiply the partial derivative of potential temperature with respect to pressure ($\equiv -T\partial \ln\theta/\partial p$), which is isobaric form of the thermodynamic equation.

4.3 Development of Statistical Model

4.3.1 Predictors

In chapter 3, the KN-MDR area for zonal-wind shear and KN-MDR or KN-NATL area for SST were selected as the best predictors for the mult-variate regression model based on their empirical relationship with the observed number of Atlantic hurricanes. In this research, static stability parameter (Sp) is added as a new predictor for the reconstruction and forecast of Atlantic hurricanes. Sensitivity experiments to select a suitable pressure level and geographic averaging domain for Sp are conducted. The reconstruction of hurricane counts with the Sp effect is used to choose an optimal SST averaging domain (KN-MDR or KN-NATL).

The vertical profiles of Sp averaged for the areas of KN-MDR, KN-NATL, VS-MDR, and VS-MDR-Wlat over the Atlantic for the period 1958-2005 are displayed in Fig. 4.1. All areas are defined in Figure. 3.1 and VS-MDR-Wlat (300ºE-340ºE, 10ºN-20ºN) is the area having a somewhat wider latitudinal domain than the VS-MDR area (300ºE-340ºE, 8ºN-15ºN). At the 850 and 200 hPa vertical levels, the KN-MDR region

static stability in years with more major hurricane (more than 5) is smaller than in years with fewer major hurricane (less than 2), indicating higher static instability in both the lower and upper troposphere is linked with intense hurricanes (Fig.4.1a). Note, low static stability is a necessary condition for TC intensification, as it sustains deep convection (DeMaria et al. 2001; Shen et al. 2000; Emanuel 1986; Holland 1997). As the 850 hPa static stability in the KN-MDR region is notably smaller than in the other three regions (KN-NATL, VS-MDR, and VS-MDR-Wlat; cf. Figs.4.1b-d), it seems reasonable to choose this pressure level and region as the optimal Sp predictor. The correlation coefficient (and p-value) between the time series of Sp from atmospheric reanalyses and the observed major Atlantic hurricane counts is noted in Table 4.1; the sensitivity analysis corroborates the predictor level and region choice as the 850 hPa Sp over the KN-MDR region has the strongest correlation (–0.572, statistically significant at 95%).

The reconstruction of major Atlantic hurricane counts with predictors from atmospheric reanalyses and SST data sets is shown in Table-4.2. The reconstruction sensitivity suggests that the KN-MDR SST (not KN-NATL SST) are more influential, both with and without the Sp influence. Inclusion of the Sp effect improves count reconstruction as evident from higher correlation and decreased RSME. Based on these sensitivity experiments, the KN-MDR Uz, KN-MDR SST, and KN-MDR Sp are selected as optimal predictors for the statistical modeling of Atlantic hurricane activity.

4.3.2 Best Subset Regression

The reconstruction of Atlantic hurricanes in Chapter 3 targeted the long-term trend in hurricane counts, and as such, were based on the IPCC-AR5 *ensemble-mean* simulations and projections. Using predictors from the ensemble-mean

simulations/projections helped minimize the interannual-to-decadal fluctuations, and their potential aliasing of the long-term count trends. Not surprisingly, the correlation of reconstructed and observed counts was rather modest (0.46, RMSE 2.45), and markedly lower in comparison with those reconstructed from observation (0.72, RMSE 1.84); see Figure 3.4.

In view of this chapter's focus on the reconstruction and prediction of the interannual-to-decadal variations of hurricane counts, it seeks to mine the rich temporal variability manifest in the ensemble members. The new statistical model (for each AR5 model) seeks an optimum set of predictors from all the ensemble simulations of that model, using the best subset technique. Best-subsets regression generates regression models using maximum R^2 criterion – indicating how much variation in the response is explained by the model; the higher the R^2, the better the model fits data – by first examining all one-predictor regression models, and then investigating the two- predictor models giving the largest R^2, and so on. This process continues until a model emerges yielding a high adjusted R^2 and predicted R^2, and a small standard error of the regression (S).

Adjusted R^2 accounts for the number of factors in the model and is useful for comparing models with different numbers of predictors. Predicted R^2 indicates how well the model predicts responses for new observations; larger values of predicted R^2 indicate greater predictive ability. S is used as a measure of model fit in regression and represents the standard distance of the data values from the regression line, or the standard deviation of the residuals. Additional information about statistical terms and formulae is provided in Appendix A.

4.3.3 Model Validation

In regression analysis, multicollinearity refers to the correlation among predictors. Moderate multicollinearity may not be problematic. However, severe multicollinearity is problematic because it can increase the variance of the regression coefficients, making them unstable and difficult to interpret. To measure mlticollinearity, the variance inflation factor (VIF) is examined, which measures how much the variance of an estimated regression coefficient increases if predictors are correlated. If the VIF is equal to 1, then there is no multicollinearity but if the VIF is more than 1 and less than 5, then predictors may be moderately correlated. When the VIF is more than 5, the regression coefficients are poorly estimated.

In choosing the best model between competing multiple regression models, Mallows' Cp (process capability statistic) provides a basis for selection, comparing the precision and bias of models with the best subset of predictors to the full model using all predictors. Mallow’s Cp is also helpful in model bias evaluation. A model with too many predictors can be relatively imprecise while one with too few can produce biased estimates. A Mallows' Cp value that is close to the number of predictors plus the constant indicates that the model is relatively precise and unbiased in estimating the true regression coefficients and predicting future responses.

If the statistical model will be used to make forecasts, cross-validation is needed. Cross-validation is a procedure to assess how well a prediction algorithm (whether or not it involves model selection) will do in forecasting the unknown future. The cross-validation typically involves withholding a data segment, developing the algorithm on the remaining data, then using the algorithm to make a prediction for the withheld period.

The result is an estimate of the out-of-sample error that more closely represents the actual forecast error when the model is used in prediction mode.

An additional issue needing consideration is overfitting of data. This generally occurs when a model is excessively complex, such as having too many predictors relative to the number of observations. A model that has been overfitted will generally have poor predictive performance, as it can exaggerate minor fluctuations in the data. A cross-validation analysis is conducted to assess the degree of degradation from potential overfitting of the model. All values of correlation coefficients and linear trends are validated by student's t-test at 95% significance level. Additional information about statistical terms and formulae is provided in Appendix A.

4.4 Reconstruction of Atlantic Hurricane Activity based on IPCC-AR5 Simulations

Based on correlation analysis, KN-MDR for the zonal-wind shear, KN-MDR for SST, and KN-MDR for Sp are chosen as optimal predictors for building the improved hurricane statistical model. The predictors are obtained from observational data (atmospheric reanalyses, SSTs) and three IPCC-AR5 models (CCSM4.0, HadCM3.0, and MPI-ESM-LR) in both the reconstruction/training period (1958-2005) and the independent forecast period (2006-2010); the GFDL-CM3.0 and MRI-CGCM3.0 data are available in the reconstruction period but not in the forecast period, and as such not used in subsequent analysis.

From the best subset regression analysis and statistical model validation, a best subset of predictors is identified for each AR5 model simulations; the number of selected

ensemble member predictors for each variable is noted for each IPCC-AR5 model in Table-4.3. It is reassuring that only a small number of ensemble predictors (less than one-third of the available) are generally used in the statistical reconstructions of all-hurricane (AH) and major hurricane (MH) counts; the one exception in the reconstruction with the Sp effect, based off CCSM4.0 data. Note, a model with too many predictors (i.e., over-fitting) can lead to poor predictions in the independent period. In reconstruction for AH and MH counts, the same predictor set (zonal-wind shear and SST) is used for reconstruction both with Sp (SP) and without the Sp (NOSP) effect, facilitating a clear analysis of the Sp effect on Atlantic hurricane counts.

The performance of the newly constructed statistical model (KN-SM_{NEW}) is compared with that of the old model (KN-SM_{OLD}) in Table-4.4. For both AH and MH, the KN-SM_{NEW} model leads to notably improved reconstruction, i.e., higher correlation and smaller RMSE, in comparison with those from the KN-SM_{OLD} model. On average (across 3 IPCC models), the KN-SM_{NEW} does even better: improves the reconstruction-observation count-correlation by 49.0% (52.3%) and decreases RMSE by 9.6% (11.8%) in the NOSP (SP) based reconstructions for AH (the second row). In addition, the KN-SM_{NEW} with SP more precisely simulates both AH and MH than the KN-SM_{NEW} NOSP does, with an increase of correlation by 12.8% (8.0%) and a decrease of RMSE by 5.1% (2.9%) for AH (MH).

The time series of the Multivariate ENSO Index (MEI) and the Atlantic hurricane counts (AH and MH) are shown together with those constructed statistically from observational data and three IPCC-AR5 models in the reconstruction period (1958-2005) in Figures 4.2 for AH and 4.3 for MH, respectively. In all reconstruction, the KN-

MDR Uz, the KN-MDR SST, and the KN-MDR Sp are used as the predictors, and the KN-SM_{NEW} is used on account of its improved performance (cf. Table-4.4). Both the reanalysis and IPCC-models based reconstructions successfully capture the variation of observed hurricane counts: the correlation and RMSE is 0.75 (1.76) for the observation based and 0.74 (1.76) for three IPCC models based AH reconstruction, and 0.77 (1.18) and by 0.67 (1.38) for MH reconstruction. The long-term linear trend in counts is however significantly steeper in the model based reconstruction: +7.52 for AH and +4.37 for MH in comparison with observations (+4.88 for AH and +2.07 for MH); all in units of counts/century.

The linkage of MEI with the observed and reconstructed AH and MH counts highlights the counteracting relationship between ENSO and Atlantic hurricane activity. Note, major land-falling hurricanes increase almost three-fold during La Niña events relative to El Niño events (Gray 1984; Bove et al. 1998). During El Niño seasons, upper-level winds from the west increase wind shear over the Atlantic MDR (Goldenberg and Shapiro 1996), making conditions less favorable for both TC genesis and intensification.

- For the five strong El Niño years (1965-1966, 1972-1973, 1982-1983, 1991-1992, and 1997-1998) depicted by MEI in the period 1958-2005, statistical count reconstruction from observations and IPCC models successfully models the strikingly below-normal AH and MH counts, but for the 1997-1998 event (which is above-normal in the KN-SM_{NEW} reconstruction).
- For five strong La Niña years (1973-1974, 1975-1976, 1988-1989, 1998-1999, and 1999-2000), AH counts are above-normal in only two of the five events (1998-1999 and 1999-2000) and MH counts above normal in four of the five

strong La Niña events (1975-1976, 1988-1989, 1998-1999, and 1999-2000). Count reconstruction from both observed and IPCC model based predictors well model the observed AH and MH count anomalies.

4.5 Forecast of Atlantic Hurricane Activity based on IPCC-AR5 Projections

As noted earlier, the prediction skill of a statistical model is likely dependent on its performance in the reconstruction/training period. The improved statistical model, KN-SM_{NEW} with predictors of zonal wind shear, SST, and Sp, was notably successful in reconstructing Atlantic hurricane counts in the training period 1958-2005. Atlantic hurricane activity is predicted for the 5-year (2006-2010) independent period with predictors from two different IPCC-AR5 data sets: the RCP4.5 projections and the Decadal 2005 predictions.

Table-4.5 shows the 5-year (2006-2010) forecast performance for AH and MH counts for the KN-SM_{NEW} based on both the RCP4.5 and Decadal 2005 (DEC2005) predictors. In both AH and MH predictions, the RCP4.5 based predictions are sub-par, i.e., poor forecast performance with low (and even negative) correlations (and high RMSE) with observed counts for two of three IPCC models: CCSM4 [–0.44 (4.54) for AH and –0.12 (2.31) for MH] and HADCM3 [0.10 (3.63) and –0.21 (2.33)]. In contrast, statistical forecasts based on predictors from the IPCC DEC2005 experiments (where the ocean state was initialized in 2005) exhibit high accuracy for both AH and MH counts in two IPCC models: CCSM4 [0.95 (3.01) for AH and 0.62 (2.29) for MH] and HADCM3 [0.96 (2.63) and 0.99 (1.57)]. However, for the MPI-ESM-LR model, the RCP4.5 forecast are slightly more accurate.

As the forecasts based on RCP4.5 and DEC2005 predictors are generated from the same statistical model, the difference in prediction outcomes must necessarily result from predictor differences. As noted earlier, the ocean-state initialization in the DEC2005 experiment must nudge the coupled climate system closer to its observed state in comparison with the RCP4.5 state where the only reference to real time is through external forcing specification (GHG concentrations, volcanoes etc.). On account of low-frequency internal climate variability, the 2006-2010 climate state in the RCP4.5 integration need not bear any resemblance to the observed state, making predictions based on the RCP4.5 state challenging.

Note, RCP4.5 is initialized with the end year-state of the IPCC-AR5 historical simulations and forced with doubling carbon dioxide concentrations by the RCP4.5 scenario, while DEC2005 is initialized with the observed ocean state in 2005 (decadal2005) and with no further increases in GHG concentrations over the 10-year (2006-2015) integration

To investigate the possibility of additional prediction improvements for Atlantic hurricane counts, a weighted Multi-Model Ensemble (3-IPCC MME) is constructed from reconstruction results, and applied to the Atlantic hurricane counts predictions generated from the same IPCC models; the weighting coefficients for three IPCC models in 3-IPCC MME is thus the same in both reconstruction and prediction. Alll forecasted Atlantic hurricane counts are verified to be statistically significant through student t-test with a 95% significance level.

The Atlantic hurricane count difference between the 2006-2010 pentad-mean and the 48-year climatology (1958-2005) is displayed in Figure 4.5. The pentad-mean AH

and MH count anomalies are positive (0.72 and 0.74, respectively) in the forecast period vis-à-vis the 48-year climatology. Overall, the pentad count prediction by the observation and IPCC-based statistical models show an increase in the pentad-mean hurricane counts, in accord with validating observations. In only one case (CCSM4), however, the pentad mean counts during the forecast period were decreased with negative anomalies in both RCP4.5 and DEC2005. It is noteworthy that the 3-IPCC MME more accurately captures the increase of observed Atlantic hurricane counts in both AH and MH during the forecast period than the observation based statistical model.

Table-4.6 provides a quantitative comparison of the KN-SM_{NEW} hurricane count forecast with the 2002-2009 forecasts produced by other groups. The data for these other hurricane forecasts comes from Kim and Webster (2010): Kim and Webster 2010 (KW, statistical model driven by ECMWF seasonal forecasts of wind shear); Colorado State University (CSU, statistical model), NOAA (http://www.cpc.noaa.gov/products/outlooks/hurricane-archive.shtml; statistical model); Tropical Storm Risk (TSR, http://www.tropicalstormrisk.com; statistical model); and ECMWF dynamical forecast for the 8 years from 2002 to 2009. The performance of the KN-SM_{NEW} model cannot be strictly compared as it produces forecasts for only 4 (2006-2009) of these 8 years; the remaining 4 are reconstructions. Notwithstanding this caveat, the KN-SM_{NEW} appears competitive and promising given its high correlation (0.90) and low RMSE (1.70), respectively.

4.6 Summary and Concluding Remarks

Atlantic hurricane counts for the Saffir-Simpson category storms 1 to 5 (all hurricanes: AH) and 3 to 5 (major hurricanes: MH) has been modeled in the reconstruction/training period (1958-2005) and forecasted in the independent period (2006-2010) with the newly developed statistical model, KN-SM$_{NEW}$. A new thermodynamic predictor, static stability parameter (Sp) in MDR region, was used to develop and improved statistical model for the Atlantic hurricane counts, both AH but MH counts. From the use of two (zonal wind shear and SST) and three (static stability, additionally) in statistical modeling, the considerable influence of Sp in count reconstruction is documented.

The goal of this chapter was to move beyond the modeling of the long-term trend in hurricane counts (Chapter 3 objective) – to modeling the interannual-to-decadal variability in hurricane counts in order to advance decadal prediction of Atlantic hurricane counts. In addition to inclusion of the third predictor (Sp), an attempt was made to capitalize on the rich temporal variability of the three predictors in the IPCC-AR5 ensemble members during statistical model development. This was accomplished through the use of the best subset regression technique which can, in principle, tap predictor values from all ensemble members; in practice, only a third were found useful in generating a credible model for both long-term trend, and interannual-to-decadal variability of counts.

The performance of the new 3-predictor, best subset regressions based statistical model (KN-SM$_{NEW}$) was compared with the previously developed model and

the extent of improvement – substantial – documented. Atlantic hurricane forecasts for the independent period 2006-2010 were generated using the new model with predictors from both IPCC-AR5 21st century (RCP4.5) projections and Decadal 2005 decadal predictions. The new model's performance was also compared with other group's forecasts in the period 2002-2009.

Overall, the key results can be summarized as follow:

- The atmospheric thermodynamic environment over KN-MDR area (270ºE-313ºE, 7ºN-15ºN) is more unstable at the 850 hPa vertical level in years with more major hurricanes. The Sp value during the active years is discernibly smaller than during years with few major hurricanes.
- The newly developed statistical model (3 predictors and best subset regressions) KN-SM_{NEW} based on three leading IPCC-AR5 models significantly improves the reconstruction performance compared to the KN-SM_{OLD} used in chapter 3 (averaged for NOSP and SP, about 51% correlation increase and 11% RMSE decrease for AH reconstruction; about 64% correlation increase and 9% RMSE decrease for MH reconstruction). In addition, the Sp predictor plays an important role in enhancing the reconstruction performance by KN-SM_{NEW} for both AH and MH (about 13% correlation increase and 5% RMSE decrease for AH reconstruction; about 8% correlation increase and 3% RMSE decrease for MH reconstruction).
- For five strong El Niño years for the period 1958-2005, the reconstructions by KN-SM_{NEW} successfully reconstructed the strikingly below normal anomalies of the observed AH and MH, excluding one event in the period 1997-1998. For five

strong La Niña years, the reconstructions based on the IPCC model predictors well reproduced the below-normal anomalies of the observed AH and MH.

- In the 5-year (2006-2010) forecasts for AH and MH, the DEC2005 predictor based statistical model has superior forecast performance in two of three IPCC models (CCSM4 and HADCM3); with RCP4.5 predictors, the model performance was unsatisfactory.
- The 3-IPCC Multi-Model Ensemble (MME) forecast for AH and MH counts, built from count forecasts from the IPCC RCP4.5 and DEC2005 predictors, is reasonably successful in predicting the increase of observed Atlantic hurricane counts in the independent period. The RCP4.5 based forecast overestimates while the DEC2005 one underestimates the counts in the forecast period 2006-2010.
- The KN-SM_{NEW} model's skill in forecasting Atlantic hurricane counts in the 2002-2009 period was compared with those of other groups. Although strict comparisons are not possible because the KN-SM_{NEW} model produces forecasts for only 4 (2006-2009) of these 8 years (the remaining 4 are reconstructions), the KN-SM_{NEW} appears competitive and promising given its high correlation (0.90) and low RMSE (1.70), respectively.

In conclusion, the newly developed statistical model, KN-SM_{NEW}, significantly improves the reconstruction and forecast of not only all-hurricane counts but also major hurricane counts.

4.7 Tables

Table-4.1: Correlation coefficients and p-value between the time series of Sp of reanalyses and the major Atlantic Hurricanes observation; the area averaged Sp is averaged from July to October (JASO) over the periods 1958-2005. The highest correlation coefficient and the lowest p-value are shown in red. The area and vertical level for Sp corresponding to the highest correlation are bold-faced.

Area	Static Stability Parameter			
	Sp850	Sp700	Sp500	Sp200
KN-MDRsst	-0.572 (0.000)	0.039 (0.791)	0.357 (0.013)	-0.440 (0.002)
KN-NATLsst	0.057 (0.699)	0.179 (0.224)	0.170 (0.247)	-0.094 (0.526)
VS-MDRuz	-0.312 (0.031)	-0.100 (0.497)	0.306 (0.034)	-0.301 (0.038)
VS-MDR-Wlat	-0.202 (0.168)	-0.122 (0.407)	0.337 (0.019)	-0.321 (0.026)

Table-4.2: Correlation coefficients, p-value, and RMSE between the time series of the observed major Atlantic hurricanes and the reconstruction from reanalyses; the predictors of wind shear, SST, and Sp are averaged from July to October (JASO) over the periods 1958-2005. The highest correlation coefficient and the corresponding p-value and RMSE are shown in red. The areas for predictors of zonal-wind shear, SST, Sp corresponding to the highest correlation coefficient are bold-faced. All correlation coefficients are statistically significant at 95% significance level (p-value < 0.05).

Predictors			CORR (p-value)	RMSE
Uz	SST	Sp850		
KN-MDR	KN-NATL	NOSP	0.735 (0.000)	1.260
		$KN\text{-}MDR_{SST}$	0.770 (0.000)	1.187
	KN-MDR	NOSP	0.742 (0.000)	1.246
		$KN\text{-}MDR_{SST}$	**0.773 (0.000)**	**1.178**

Table-4.3: Numbers of ensemble members of each IPCC-AR5 model used in the reconstruction of all Atlantic hurricanes (AH) and major hurricanes (MH) for the period 1958-2005. Numbers of all available ensemble members for each IPCC model are bold-faced; the members used in the reconstruction of AH (blue) and MH (red). The experiment including (excluding) Sp predictor is denoted by SP (NOSP).

IPCC-AR5 MODELS		CC SM4.0				HADCM3.0				MPI-ESM-LR			
Predictor		Uz	SST	Sp	**Tot**	Uz	SST	Sp	**Tot**	Uz	SST	Sp	**Tot**
All Ensemble Members		6	6	6	**18**	10	10	10	**30**	3	3	3	**9**
All Hurricanes (AH)	NOSP	3	3		**6**	1	3		**4**	1	1		**2**
	SP	3	3	4	**10**	1	3	1	**5**	1	1	1	**3**
Major Hurricanes (MH)	NOSP	1	4		**5**	1	3		**4**	1	1		**2**
	SP	1	4	1	**6**	1	3	1	**5**	1	1	1	**3**

Table-4.4: Correlation coefficients and RMSE between the time series of the reconstruction and observed all Atlantic hurricanes (AH, the second row) and major hurricanes (MH, the third row) from three IPCC-AR5 models over the period 1958-2005. The reconstruction by using the statistical model built earlier − based on the average of ensemble members − is denoted by KN-SMOLD; and the models developed by best subset technique is marked by KN-SMNEW (blue). The percentile SP effect is calculated from the correlation and RMSE values between NOSP and SP within a homogeneous statistical model for AH and MH, respectively. The extent of improvement by KN-SMNEW is calculated from the correlation and RMSE values between KN-SMOLD and KN-SMNEW within a homogeneous SP option for AH and MH, respectively (red).

	EXP. SETS		CCSM4	HADCM3	MPI-ESM-LR	AVERAGE
AH	$KN\text{-}SM_{OLD}$	NOSP	0.37 (2.45)	0.35 (2.47)	0.33 (2.49)	-
		SP	0.37 (2.45)	0.35 (2.47)	0.48 (2.31)	-
		SP effect (%)	0.0 (0.0)	0.0 (0.0)	45.5 (-7.2)	15.2 (-2.4)
	$KN\text{-}SM_{NEW}$	NOSP	0.55 (2.20)	0.62 (2.08)	0.40 (2.42)	-
		SP	0.67 (1.96)	0.63 (2.06)	0.46 (2.34)	-
		SP effect (%)	21.8 (-10.9)	1.6 (-1.0)	15.0 (-3.3)	12.8 (-5.1)
	$KN\text{-}SM_{NEW}$ Improvement (%)	NOSP	48.6 (-10.2)	77.1 (-15.8)	21.2 (-2.8)	49.0 (-9.6)
		SP	81.1 (-20.0)	80.0 (-16.6)	-4.2 (1.3)	52.3 (-11.8)
MH	$KN\text{-}SM_{OLD}$	NOSP	0.30 (1.78)	0.34 (1.75)	0.19 (1.82)	-
		SP	0.31 (1.77)	0.34 (1.75)	0.38 (1.72)	-
		SP effect (%)	3.3 (-0.6)	0.0 (0.0)	100 (-5.5)	34.4 (-2.0)
	$KN\text{-}SM_{NEW}$	NOSP	0.48 (1.64)	0.56 (1.54)	0.38 (1.72)	-
		SP	0.54 (1.57)	0.61 (1.48)	0.39 (1.71)	-
		SP effect (%)	12.5 (-4.3)	8.9 (-3.9)	2.6 (-0.6)	8.0 (-2.9)
	$KN\text{-}SM_{NEW}$ Improvement (%)	NOSP	60.0 (-7.9)	64.7 (-12.0)	100.0 (-5.5)	74.9 (-8.5)
		SP	74.2 (-11.3)	79.4 (-15.4)	2.6 (-0.6)	52.1 (-9.1)

Table-4.5: Correlation coefficients and RMSE between the time series of the forecast from three IPCC-AR5 models and observed Atlantic hurricanes (AH, the second row and MH, the third row) over the period 2006-2010. The forecast based on RCP4.5 is denoted by RCP4.5; and based on decadal experiment is marked by DEC2005 (blue).

EXP. SET		CCSM4	HADCM3	MPI-ESM-LR
AH	RCP4.5	-0.44 (4.54)	0.10 (3.62)	0.68 (2.67)
	DEC2005	0.95 (3.01)	0.96 (2.63)	0.24 (2.98)
MH	RCP4.5	-0.12 (2.31)	-0.21 (2.33)	0.88 (1.04)
	DEC2005	0.62 (2.29)	0.99 (1.57)	0.49 (1.44)

Table-4.6: Comparison for the number of forecasted all Atlantic hurricane counts issued by several groups' hurricane forecast model from 2002 to 2009*: Colorado State University (CSU), NOAA, NCEP's Climate Forecast System (CFS), Tropical Storm Risk (TSR), and ECMWF. To compare the performance of forecast, correlation coefficients and RMSE for each model's forecast with the observed Atlantic hurricane counts are calculated over the period. For NOAA forecast, an average of the minimum and maximum counts is used for the calculation of correlation coefficient and RMSE.

Year Issue	OBS	KN-SM$_{NEW}$	KW	CSU	NOAA	CFS	TSR	ECMWF
2002	4	6	3	4	4-6	4	4	5
2003	7	6	7	8	7-9	7	7	8
2004	9	10	8	7	6-8	7	8	5
2005	15	12	9	10	9-11	11	11	8
2006	5	5	7	7	7-9	9	8	13
2007	6	6	7	8	7-9	9	8	7
2008	8	6	9	9	7-10	9	10	9
2009	3	5	5	4	3-6	5	7	4
CORR		0.90	0.75	0.80	0.73	0.73	0.76	0.15
RMSE		1.70	2.45	2.24	2.41	2.50	2.50	4.09

*Numbers are rounded to the nearest integer. RMSE are on the bottom.

4.8 Figures

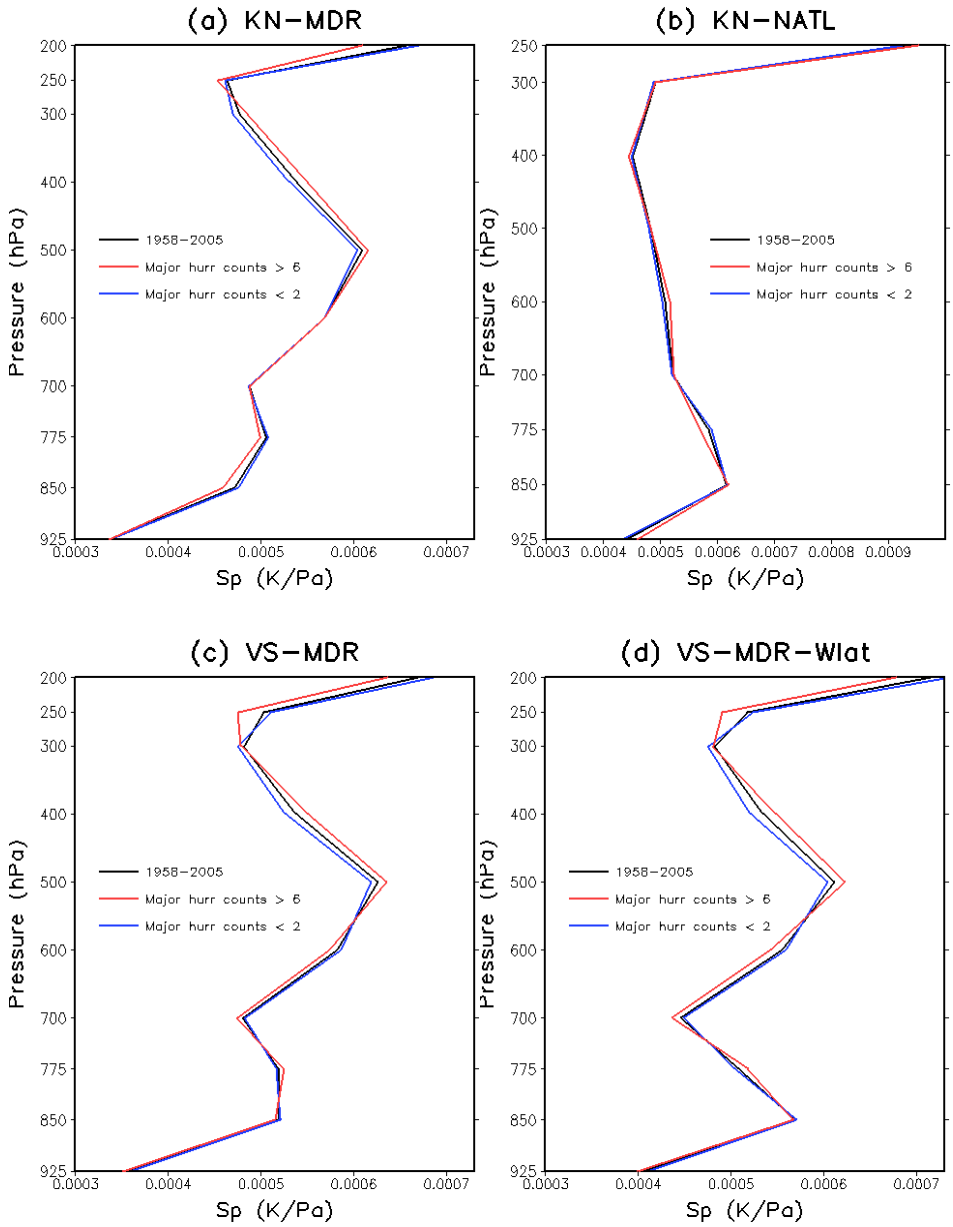

Figure 4.1: Vertical profiles of static stability parameter (Sp) averaged over the area of (a) KN-MDR SST, (b) KN-NATL SST, (c) VS-MDR Uz, and (d) VS-MDR-Wlat Uz. The 48-year (1958-2005) climatological Sp profile is shown in black; the profile of Sp averaged for the years recorded more (less) than five (two) major Atlantic hurricane counts is shown in red (blue). All areas excluding VS-MDR-Wlat are defined as in Figure 3.1; VS-MDR-Wlat is defined over the area of 300ºE-340ºE, 10ºN-20ºN.

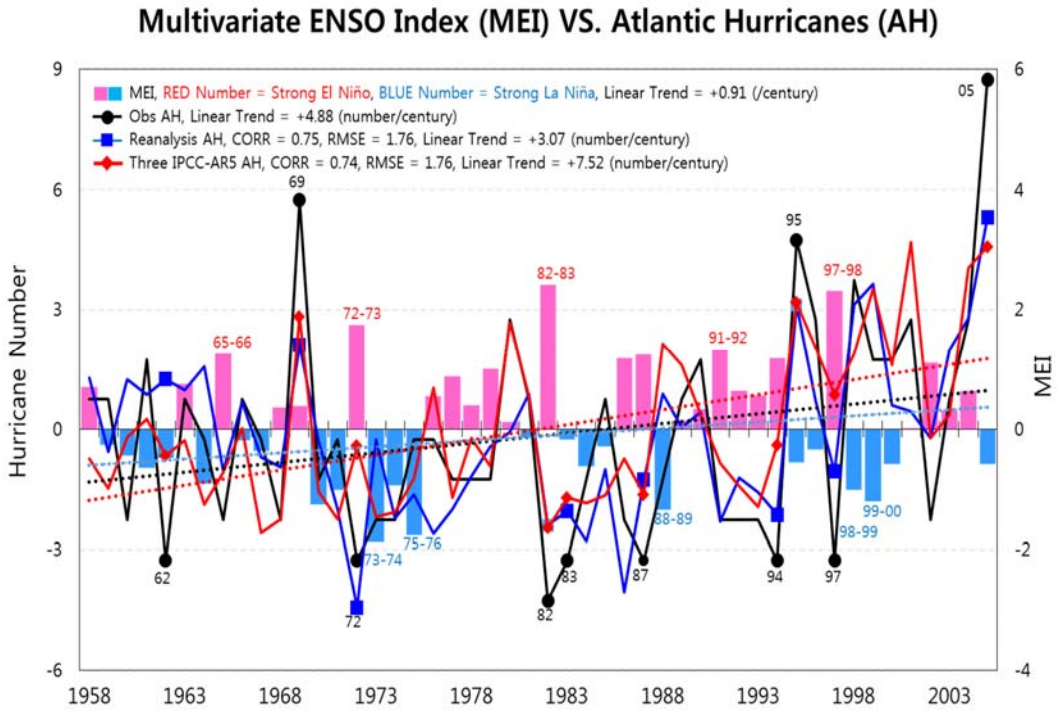

Figure 4.2: The time series of MEI and the anomaly of observed all atlantic hurricanes for the period 1958-2005 (black-solid), the reconstruction from reanalyses (blue-solid), and three IPCC-AR5 models (red-solid); the corresponding correlation coefficients, RMSE, and linear trend values are noted in the legend. The above (below) normal MEI is displayed with pink bar (light blue bar) and the years of strong El Niño (La Niña) are denoted by red (light blue). Remarkably anomalous years corresponding to integer hurricane number more than +4 (less than -3) are depicted in balck-dot, blue-rectangle, and red-diamond.

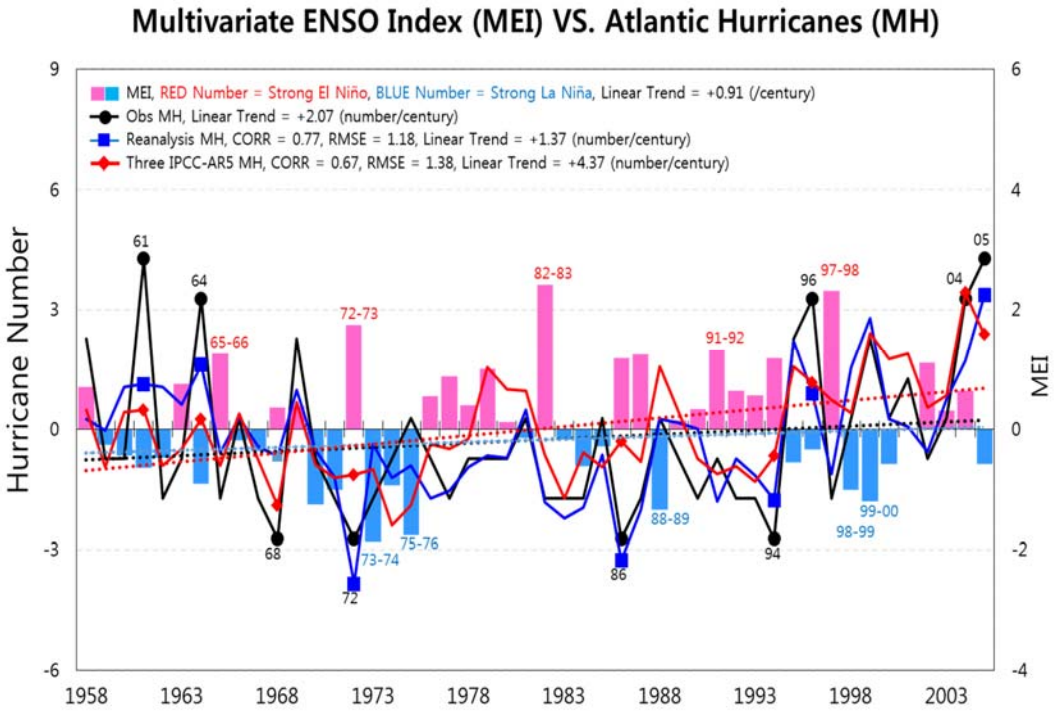

Figure 4.3: As in Figure 4.2 but for the time series from major Atlantic hurricanes. Remarkably anomalous years corresponding to integer hurricane number more than +3 (less than -2) are depicted in balck-dot, blue-rectangle, and red-diamond.

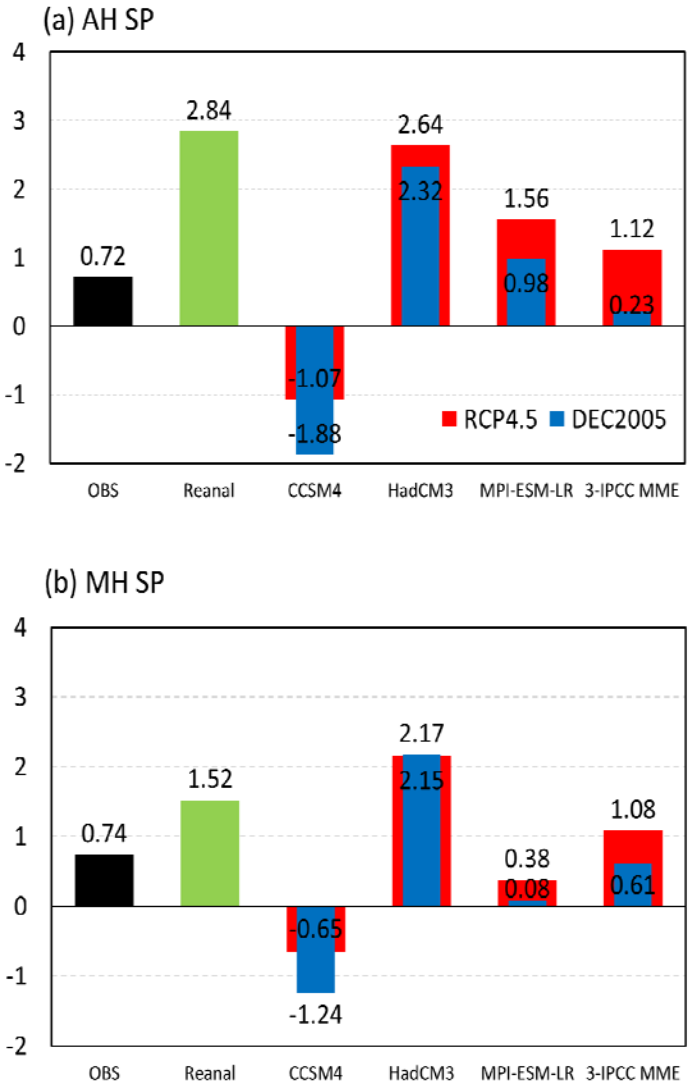

Figure 4.4: The difference of Atlantic hurricane counts between 5-year average for the period 2006-2010 and 48-year climatology for the period 1958-2005: for all hurricanes (a) AH SP (upper panel) and major hurricanes (b) MH SP (lower panel). Pentad prediction by the best subset regression model is from each of three IPCC models and a weighted multi-model ensemble of three IPCC models (3-IPCC MME). The counts difference corresponding to observation, reanalyses, RCP4.5, and DEC2005 is denoted with bars in black, green, red, and blue, respectively.

Chapter 5: Science Questions and Answers, and Future Work

5.1 Science Questions and Answers

- *Does unequivocal evidence exists for increasing vertical wind-shear in the tropical Atlantic under climate warming scenario in 21st century?*

  NO compelling case for a statistically significant positive vertical wind-shear over MDR in IPCC-AR4 and AR5 simulations/projections– in contrast with claims based on indiscriminate multi-model averaging (e.g., Vecchi and Soden 2007).

- *Can the trend in Atlantic hurricane counts be modeled from variations in regional wind shear and SST?*

  Yes, quite effectively. Optimal predictors for hurricane counts – definition and averaging domain – were determined from correlation and linear regression analyses: Uz, SST, and Sp. The long-term (1958-2005) trend in counts successfully modeled with both observations and IPCC-AR5 ensemble-mean simulation based predictors.

- *Can this modeling approach provide insights into the long-term trend in counts in the 20th and 21st century climate? Which variations (e.g., SST, wind shear) are more influential?*

  Yes. Statistical modeling based on IPCC-AR5 20C simulations indicates the increasing trend in hurricane counts to arise primarily from the SST influence. Statistical models that generate realistic count-trends in the 20th century project a

somewhat stronger trend in counts with predictors from IPCC-AR5 21C projections.

- *Can the statistical model for Atlantic hurricane counts be improved to account for interannual-to-decadal count variations?*

  Yes, from consideration of complex variability manifest in the IPCC-AR5 20C simulation ensembles, through the best subset regression approach. Best subset regression modeling yields correlations of 0.46-0.67 between reconstructed and observed counts; a weighted multi-model averaging of statistical reconstruction yields even higher correlation (0.74) and lower RMSE.

- *Can this improved statistical model be used for decadal prediction of counts?*

  Perhaps, yes. There are not enough independent prediction periods with validating observations to make the assessment. Preliminary analysis of the 2006-2010 annual and pentad predictions based on IPCC Decadal 2005 (ocean initialized) experiments indicates that the weighted multi model statistical predictions have some potential.

5.2 Future Work

The outcome of this work, despite several known limitations, advance understanding and statistical modeling of Atlantic hurricane counts. In Chapter 4, the well-known link of Atlantic hurricane activity with ENSO was further analyzed, and reconstructed using related environmental fields. The relationship is of obvious interest since statistically based seasonal forecasts of tropical cyclone activity in the western North Pacific use ENSO as one of the main predictors (Chan et al. 1998; 2001).

Grounded in the link between ENSO and Atlantic/Pacific hurricane activity, and the empirical relationship between environmental variables and hurricane activity, and encouraged by the striking performance of the statistical model developed in this thesis, it would be of considerable interest to reconstruct and predict variations in western North Pacific Typhoon (WNP-TY) activity. Specifically, future research lines include:

- Investigation of the change in environmental factors such as wind shear, SST, and static stability over WNP in the 20th and 21st centuries;
- Analyze the linkage between MEI and WNP-TY in the 20th and 21st centuries;
- Advance the understanding of how environmental factors and MEI affect WNP-TY activity under a warming climate;
- Develop a statistical WNP-TY prediction model based on empirical relationships with environmental factors ; and
- Provide the evidence of the change of WNP-TY activity in the 21st century and its decadal predictability

Appendix A: Statistical Techniques and formulae

A.1 R-Squared (R^2)

R-squared indicates how much variation in the response is explained by the model. The higher the R^2, the better the model fits your data. The formula is:

$$R^2 = 1 - \frac{\sum (y_i - \hat{y}_i)^2}{\sum (y_i - \overline{y}_i)^2}$$

Where,

y_i = i[th] observed response value

$\hat{y}_i$ = i[th] fitted response

$\overline{y}_i$ = mean response

Percentage of response variable variation that is explained by its relationship with one or more predictor variables. In general, the higher the R^2, the better the model fits your data. R^2 is always between 0 and 100%. It is also known as the coefficient of determination or multiple determination (in multiple regression).

A.2 Adjusted R-Squared (R^2)

Adjusted R^2 accounts for the number of factors in your model and is useful for comparing models with different numbers of predictors. The formula is:

$$R^2_{adj} = 1 - \frac{\sum (y_i - \hat{y})^2}{\sum (\hat{y}_i - \overline{y})^2} \left(\frac{n-1}{n-p-1}\right)$$

Where,

y_i = ith observed response value

$\hat{y}_i$ = ith fitted response

$\overline{y}_i$ = mean response

N= number of observations

P= number of terms in the model

Percentage of response variable variation that is explained by its relationship with one or more predictor variables, adjusted for the number of predictors in the model. This adjustment is important because the R^2 for any model will always increase when a new term is added. A model with more terms may appear to have a better fit simply because it has more terms. However, some increases in R^2 may be due to chance alone. The adjusted R^2 is a useful tool for comparing the explanatory power of models with different numbers of predictors. The adjusted R^2 will increase only if the new term improves the model more than would be expected by chance. It will decrease when a predictor improves the model less than expected by chance.

A.3 Predicted R-Squared (R^2)

Predicted R-squared indicates how well the model predicts responses for new

observations. Larger values of predicted R^2 suggest models of greater predictive ability. The formula is:

$$R^2_{pred} = \frac{\sum (\frac{e_i}{1-h_i})^2}{1-\sum (y_i - \bar{y})^2},$$

Where,

e_i = i^{th} observed response value

h_i = i^{th} diagonal element of $X(X'X)^{-1}X'$, X=predictor matrix, X'=transpose of X

Predicted R-Squared is used in regression analysis to indicate how well the model predicts responses for new observations, whereas R^2 indicates how well the model fits your data. Predicted R^2 can prevent overfitting the model and can be more useful than adjusted R^2 for comparing models because it is calculated using observations not included in model estimation. Overfitting refers to models that appear to explain the relationship between the predictor and response variables for the data set used for model calculation but fail to provide valid predictions for new observations. Predicted R^2 is calculated by systematically removing each observation from the data set, estimating the regression equation, and determining how well the model predicts the removed observation. Predicted R^2 ranges between 0 and 100% and is calculated from the PRESS statistic. Larger values of predicted R^2 suggest models of greater predictive ability.

A.4 Standard error of the regression (S)

An estimate of s, the estimated standard deviation of the error in the model. Note

that s^2 = Mean Square Error (MSE).

$$S^2 = \frac{\sum (y_i - \hat{y}_i)^2}{n - p - 1}$$

Where,

y_i = i^{th} observed response value

$\hat{y}_i$ = i^{th} fitted response

n= number of observations

P= number of terms in the model

Standard error of the regression (S) is used as a measure of model fit in regression and ANOVA. S is measured in the units of the response variable and represents the standard distance data values fall from the regression line, or the standard deviation of the residuals. For a given study, the better the equation predicts the response, the lower the value of S.

A.5 Variance inflation factor (VIF)

Variance inflation factor (VIF) is used to detect multicollinearity (correlated predictors). VIF measures how much the variance of an estimated regression coefficient increases if your predictors are correlated. Minitab calculates VIF by regressing each predictor on the remaining predictors and noting the R^2 value. For predictor x1, the VIF is:

$$VIF = \frac{1}{1 - R^2(x_1)}$$

VIF = 1, Not correlated

1< VIF <5, Moderately correlated

VIF > 5, Highly correlated

VIF values greater than 10 may indicate multicollinearity is unduly influencing your regression results. In this case, you may want to reduce multicollinearity by removing unimportant predictors from your model.

A.6 Mallows' Cp

Mallow's Cp (process capability) is a measure of goodness-of-prediction. The formula is:

$$(SSEp / MSEm) - (n - 2p)$$

Where,

$SSEp = \sum (y_i - \hat{y}_i)^2$, the sum of square error for the model under consideration,

$MSEp = \frac{\sum (y_i - \hat{y}_i)^2}{n - p - 1}$, the mean square error for the model with all predictors included,

n = the number of observations,

p = the number of terms in the model, including the constant.

In general, look for models where Mallows' Cp is small and close to p. A small Cp value indicates that the model is relatively precise (has small variance) in estimating the true regression coefficients and predicting future responses. Models poor predictive ability and bias have values of Cp larger than p.

A statistic used as an aid in choosing between competing multiple regression models. Mallows' Cp compares the precision and bias of the full model to models with the best subsets of predictors. It helps you strike an important balance with the number of predictors in the model. A model with too many predictors can be relatively imprecise while one with too few can produce biased estimates. A Mallows' Cp value that is close to the number of predictors plus the constant indicates that the model is relatively precise and unbiased in estimating the true regression coefficients and predicting future responses.

Bibliography

Aiyyer AR, Thorncroft C (2006) Climatology of vertical wind shear over the tropical Atlantic. J Climate 19:2969–2983.

Aiyyer AR, Thorncroft C (2011) Interannual-to-multidecadal variability of vertical shear and tropical cyclone activity. J Climate 24: 2949–2962.

Alves OG, Wang A, Zhong N, Smith G, Warren A, Marshall F, Tzeitkin, Schiller A (2002) POAMA: Bureau of Meteorology operational coupled model season forecast system. Proc. ECMWF Workshop on the Role of the Upper Ocean in Medium and Extended Range Forecasting, Reading, United Kingdom, ECMWF: 22–32.

Bender MA (1997): The effect of relative flow on the asymmetric structure in the interior of hurricanes. J Atmos Sci 54, 703-724.

Bender MA, Knutson TR, Tuleya RE, Sirutis JJ, Vecchi GA, Garner ST, Held IM (2010) Modeled impact of anthropogenic warming on the frequency of intense Atlantic hurricanes. Science 327, 454–458.

Bengtsson L, Hodges KI, EschM, Keenlyside N, Kornblueh L, Luo JJ, Yamagata T (2007) How may tropical cyclones change in a warmer climate? Tellus 59A:539–561.

Berrisford P, Dee D, Fielding K, Fuentes M, Kallberg P, Kobayashi S, Uppala S (2009) The ERA-interim archive, ERA Rep. Ser. 1, Eur. Cent. for Medium-Range Weather Forecasts, Reading, U. K.

Burroughs WJ (2007) Climate change : a multidisciplinary approach. Cambridge: Cambridge University Press. ISBN 9780521870153

Camargo SJ, Emanuel KA, Sobel AH (2007) Use of genesis potential index to diagnose ENSO effects upon tropical cyclone genesis, J Climate 20, 4819-4834.

Chan JCL (1995) Tropical cyclone activity in the western North Pacific in relation to the stratospheric quasi-biennial oscillation. Mon Wea Rev 123, 2567–2571.

Chan JCL, Shi JE, Lam CM, Liu KS (2001) Improvements in the seasonal forecasting of tropical cyclone activity over the western North Pacific. Wea. Forecasting, 16, 491–498.

Chang EKM, Guo Y (2007) Is the number of North Atlantic tropical cyclones significantly underestimated prior to the availability of satellite observations? Geophys Res Lett 34:14801

Compo GP, Coauthors (2011), The Twentieth Century Reanalysis Project, Q. J. R. 211 Meteorol. Soc., 137, 1–28. DOI:10.1002/qj.776

Chauvin F, Royer JF, Déqué M (2006) Response of hurricane-type vortices to global warming as simulated by ARPEGE-Climat at high resolution. Clim Dyn 27:377–399

Delworth TL, Mann ME (2000) Observed and simulated multidecadal variability in the Northern Hemisphere. Clim Dyn 16:661–676

DeMaria M (1996) The effect of vertical shear on tropical cyclone intensity change. J Atmos Sci 53(14):2076–2087.

DeMaria M, Knaff JA, Connell BH (2001) A tropical cyclone genesis parameter for the tropical Atlantic. Wea. Forecasting, 16: 219–233

Elsner JB, Bossak BH, Niu XF (2001) Secular changes to the ENSO U.S. hurricane relationship. Geophy Res Lett 28:4123–4126

Emanuel KA (1986) The maximum potential intensity of hurricanes. J Atmos Sci 45, 1143–1155

Emanuel KA (1989) The finite-amplitude nature of tropical cyclogenesis. J Atmos Sci 46, 3431-3456.

Emanuel KA, Nolan DS (2004) Tropical cyclones and the global climate system, paper presented at 26th Conference on Hurricanes and Tropical Meteorology, Am. Meteorol. Soc., Miami Beach, Fla.

Emanuel KA (2005) Divine Wind: The History and Science of Hurricanes. Oxford University Press, 285 pp.

Emanuel KA (2007) Environmental factors affecting tropical cyclone power dissipation. J. Clim 20:5497–5509.

Emanuel KA, Sundararajan R, Williams J (2008) Hurricanes and global warming: Results from downscaling IPCC-AR4 simulations. Bull Am Meteorol Soc 89:347–367

Enfield DB, Mestaz-Nuñez AM, Trimble PJ (2001) The Atlantic multidecadal oscillation and its relation to rainfall and river flows in the continental U.S. Geophys Res Lett 28:2077–2080

Enfield DB, Cid-Serrano L (2010) Secular and multidecadal warmings in the North Atlantic and their relationships with major hurricane activity. Intl J Climatol 30, 174–184

Frank WM, Ritchie EA (1999) Effects of environmental flow upon tropical cyclone structure. Mon Wea Rev 127: 2044-2061.

Frank WM, Ritchie EA (2001) Effects of vertical wind shear on the intensity and structure of numerically simulated hurricanes, Mon Wea Rev 129: 2249–2269.

Garner ST, Held IM, Knutson T, Sirutis J (2009) The roles of wind shear and thermal stratification in past and projected changes of Atlantic tropical cyclone activity. J Climate 22:4723–4734.

Goldenberg SB, Shapiro LJ (1996) Physical mechanisms for the association of El Niño and West African rainfall with Atlantic major hurricane activity. J Climate 9: 1169–1187.

Goldenberg SB, Landsea C, Mestas-Nuñez AM, Gray WM (2001) The recent increase in Atlantic hurricane activity, Science 293: 474– 479.

Gray WM (1968) Global view of the origin of tropical disturbances and storms. Mon Wea Rev 96: 969-700

Gray WM (1979) Hurricanes: their formations, structure and likely role in the tropical circulation. Meteorology Over the Tropical Oceans, Royal Meteorological Society, James Glaisher House, Grenville Place, Bracknell, Berkshire, RG 12 1BX, D. B. Shaw, Ed., 155–218

Gray WM (1984) Atlantic seasonal hurricane frequency. Part I: El Niño and 30-mb quasi-biennial oscillation influences. Mon Wea Rev 112: 1649–1668.

Gray, WM (1998) The Formation of Tropical Cyclones. Meteorol. Atmos Phys 67, 37-69.

Grossmann I, Klotzbach P (2009) A review of North Atlantic modes of natural variability and their driving mechanisms. J Geophys Res 114:D24107

Gualdi S, Scoccimarro E, Navarra A (2008) Changes in tropical cyclone activity due to global warming: results from a high-resolution coupled general circulation model. J Climate 21(20):5204–5228.

Guan B, Nigam S (2009) Analysis of Atlantic SST variability factoring inter-basin links and the secular trend: clarified S. Nigam, B. Guan: Atlantic tropical cyclones in the twentieth century 123 structure of the Atlantic multidecadal oscillation. J Climate 22:4228–4240

Holland G (1997) The maximum potential intensity of tropical cyclones. J Atmos Sci 54: 2519–2541

Holland GJ, Webster PJ (2007) Heightened tropical cyclone activity in the North Atlantic: natural variability or climate trend? Philos Trans R Soc London Ser A 365:2695–2716. doi:10.1098/rsta.2007.2083

Ji M, Kumar A, Leetmaa A (1994) Development of seasonal climate forecast system using coupled ocean-atmosphere model at National Meteorological Center. Bull Amer Meteor Soc 75, 569–577.

Jones SC (1995) The evolution of vortices in vertical shear. I: Initially barotropic vortices. Q.J.R. Met. Soc., 121: 821-851.

Kalnay E et al. (1996) The NCEP/NCAR 40-Year Reanalysis Project, Bull. Am. Meteorol. Soc., 77: 437–471.

Kanamitsu MW, Ebisuzaki W, Woollen J, Yang SK, Hnilo JJ, Fiorino M, Potter GL (2002) NCEP–DOE AMIP-II Reanalysis (R-2). Bull Amer Meteor Soc 83, 1631–1643.

Kim HM, Webster PJ (2010) Extended-range seasonal hurricane forecasts for the North Atlantic with a hybrid dynamical-statistical model. Geophys Res Lett 37, L21705, doi:10.1029/2010GL044792.

Klotzbach PJ (2007) Revised prediction of seasonal Atlantic basin tropical cyclone activity from

1 August, Weather Forecast., 22, 937–949, doi:10.1175/WAF1045.1.

Klotzbach PJ, Gray WM (2008) Multidecadal variability in North Atlantic tropical cyclone activity. J. Clim 21:3929–3935

Knaff JA, Seseske SA, DeMaria M, Demuth JL (2004) On the influences of vertical wind shear on symmetric tropical cyclone structure derived from AMSU. Mon Wea Rev 132: 2503-2510.

Knutson TR, Tuleya RE (2004) Impacts of CO2-induced warming on simulated hurricane intensity and precipitation: sensitivity to the choice of climate model and convective parameterization. J Climate 17(18):3477–3495

Knutson TR, Tuleya RE, Shen W, Ginis I (2001) Impacts of CO2-induced warming on hurricane intensities as simulated in a hurricane model with ocean coupling. J Climate 14:2458–2468

Knutson TR, Sirutis JJ, Garner ST, Held IM, Tuleya RE (2007) Simulation of the recentmultidecadal increase of Atlantic hurricane activity using an 18-km-grid regional model. Bull Am Meteorol Soc 88(10):1549–1565

Knutson TR, Sirutis JJ, Garner ST, Vecchi GA, Held IM (2008) Simulated reduction in Atlantic hurricane frequency under twenty-first-century warming conditions. Nature Geoscience 1:359–364

Kossin JP, Knapp JR, Vimont DJ, Murnane RJ, Harper BA (2007) A globally consistent reanalysis of hurricane variability and trends. Geophys Res Lett 34:L04815.

Kossin JP, Vimont DJ (2007) A more general framework for understanding Atlantic hurricane variability and trends, Bull. Am. Meteorol. Soc., 88: 1767–1781, doi:10.1175/BAMS-88-11-1767.

Landsea CW, Pielke RA, Mestas-Nuñez AM, Knaff JA (1999) Atlantic basin hurricanes: Indices of climate changes, Clim. Change, 42: 89– 129.

Landsea CW (2007) Counting Atlantic tropical cyclones back to 1900. Eos Trans. AGU 88(18): 197–202

Landsea CW, Vecchi GA, Bengtsson L, Knutson TR (2010) Impact of duration thresholds on

Atlantic tropical cyclone counts. J Climate 23:2508–2519

Lighthill J, Holland GJ, Gray WM, Landsea C, Emanuel K, Craig C, Evans J, Kurihara Y, Guard CP (1994) Global climate change and tropical cyclones. Bull Amer Meteor Soc 75, 2147-2157.

Mann ME, Emanuel KA (2006) Atlantic hurricane trends linked to climate change. Eos Trans AGU 87(24):233–244.

Mann ME, Emanuel KA, Holland GJ, Webster PJ (2007) Atlantic tropical cyclones revisited. Eos Trans AGU 88: doi:10.1029/2007EO360002

Marks FD (2003) Hurricanes. Encyclopedia of Atmospheric Sciences, Elsevier Science Ltd., London, UK, 942-966.

Marshall J, Kushnir Y, Battisti D, Chang P, Czaja A, Dickson R, Hurrell J, McCartney M, Saravanan R, Visbeck M (2001) North Atlantic climate variability: phenomena, impacts and mechanisms. Int. J. Climatol 21(15):1863–1898

Mason SJ, Goddard L, Graham NE, Yulaeva E, Sun L, Arkin PA (1999) The IRI seasonal climate prediction system and the 1997/98 El Niño event. Bull Amer Meteor Soc 80, 1853–1873.

McDonald RE, Bleaken DG, Cresswell DR, Pope VD, Senior CA (2005) Tropical storms: representation and diagnosis in climate models and the impacts of climate change. Clim Dyn 25:19–36

Meehl GA, Stocker TF, Collins WD, Friedlingstein P, Gaye AT, Gregory JM, Kitoh A, Knutti R, Murphy JM, Noda A, Raper SCB, Watterson IG, Weaver AJ, Zhao ZC (2007) Global climate projections. In: Climate change 2007, the physical science basis. Contributions of working group I to the fourth assessment report of the Intergovernmental Panel on Climate Change.

Nigam S, Guan B (2010) Atlantic tropical cyclones in the twentieth century: natural variability and secular change in cyclone count, Climate Dynamics, DOI 10. 1007/s00382-010-0908-x.

Pielke RA, Landsea CW (1999) La Niña, El Niño, and Atlantic hurricane damages in the United States, Bull. Am. Meteorol. Soc., 80: 2027– 2033.

Oouchi KJ, Yoshimura J, Yoshimura H, Mizuta R, Kusunoki S, Noda A (2006) Tropical cyclone

climatology in a global-warming climate as simulated in a 20 km-mesh global atmospheric model: frequency and wind intensity analysis. J Meteorol Soc Jpn 84(2):259–276

Palmer TN, Coauthors (2004) Development of a European multimodel ensemble system for seasonal-to-interannual prediction (DEMETER). Bull Amer Meteor Soc 85, 853–872.

Rotunno R, Emanuel KA (1987) An air-sea interaction theory for tropical cyclones. Part II: Evolutionary study using a non-hydrostatic axisymmetric numerical model. J Atmos Sci 44, 542-561.

Saunders MA, Lea AS (2008) Large contribution of sea surface warming to recent increase in Atlantic hurricane activity. Nature 451:557–561.

Shen W, Tuleya RE, Ginis I, (2000) A sensitivity study of the thermodynamic environment on GFDL model hurricane intensity: Implications for global warming. J Climate 13: 109121

Shultz JM., Russell J, Espinel Z (2005) Epidemiology of Tropical Cyclones: The Dynamics of Disaster, Disease, and Development. Epidemiologic Reviews 27 (1): 21–25

Smith TM, Reynolds RW (2004) Improved extended reconstruction of SST (1854–1997), J Climate 17, 2466–2477, doi:10.1175/1520-0442(2004)017<2466:IEROS>2.0.CO;2

Swanson KL (2008) Non-locality of Atlantic tropical cyclone intensities.Geochem Geophys Geosys. doi:10.1029/2007GC001844

Trenberth KE, Shea DJ (2006) Atlantic hurricanes and natural variability in 2005, Geophys Res Lett 33, L12704, doi:10.1029/2006GL026894.

Vecchi GA, Soden BJ (2007b) Increased tropical Atlantic wind shear in model projections of global warming. Geophys Res Lett 34:L08702.

Vecchi GA, Knutson TR (2008) On estimates of historical North Atlantic tropical cyclone activity. J Climate 21:3580–3600

Vimont DJ, Kossin JP (2007) The Atlantic meridional mode and hurricane activity, Geophys Res Lett 34, L07709, doi:10.1029/2007GL029683.

Vitart F, Huddleston MR, Déqué M, Peake D, Palmer TN, Stockdale TN, Davey MK, Ineson S,

and Weisheimer A (2007) Dynamically-based seasonal forecasts of Atlantic tropical storm activity issued in June by EUROSIP, Geophys Res Lett 34, L16815, doi:10.1029/2007GL030740.

Wang H et al (2009) A Statistical forecast model for Atlantic seasonal hurricane activity based on the NCEP dynamical seasonal forecast, J Climate 22, 4481–4500, doi:10.1175/2009JCLI2753.1.

Wolter K (1987) The Southern Oscillation in surface circulation and climate over the tropical Atlantic, Eastern Pacific, and Indian Oceans as captured by cluster analysis. J Climate Appl. Meteor., 26, 540-558.

Wolter K, Timlin MS (1993) Monitoring ENSO in COADS with a seasonally adjusted principal component index. Proc. of the 17th Climate Diagnostics Workshop, Norman, OK, NOAA/NMC/CAC, NSSL, Oklahoma Clim. Survey, CIMMS and the School of Meteor., Univ. of Oklahoma, 52-57

Webster PJ, Holland GJ, Curry JA, Chang HR (2005) Changes in tropical cyclone number, duration, and intensity in a warming environment. Science 309:1844–1846

World Meteorological Organization (2006) Statement on tropical cyclones and climate change. WMO 6th International Workshop on Tropical Cyclones, San Jose

Wu L, Wang B (2008) What has changed the proportion of intense hurricanes in the last 30 years. J Climate 21:1432–1439

Zhang R, Delworth TL (2006) Impact of Atlantic multidecadal oscillations on India/Sahel rainfall and Atlantic hurricanes, Geophys Res Lett 33, L17712, doi:10.1029/2006GL026267.

Zhao M, Held IM, Lin SJ, Vecchi GA (2009) Simulations of global hurricane climatology, interannual variability, and response to global warming using a 50 km resolution GCM. J Climate 22:6653–6678.

Zehr RM (1992) Tropical cyclogenesis in the western North Pacific. NOAA Technical Report NESDIS 61.